10th International Workshop on Multiple Partonic Interactions at the LHC

Effects of geometry initial state fluctuations on the ridge structure in pp collisions

Irais Bautista

FCFM-BUAP

13th December, Perugia

CONACYT

BUAP

Small systems

- In small systems, the finite-size and fluctuation effects become relevant
- Fast expansion and cooling with a lifetime of a few fm/c.

- T. S. Biro, G. G. Barnafoldi, G. Biro and K. M. Shen, J. Phys. Conf. Ser. 779 (2017) no.1, 012081
- G. Bíró, G. G. Barnaföldi, T. S. Biró and K. Ürmössy, AIP Conf. Proc 1853 (2017) 08000
- C. Gale, S. Jeon, and B. Schenke, Int. J. Mod. Phys.
- N. Armesto and E. Scomparin, Eur. Phys. J. Plus 13, 52 (2016)

Color sources

- In the transverse impact parameter plane the strings look like small disk where we can apply 2 dimensional percolation theory

$\sqrt{s}$, N_{part}

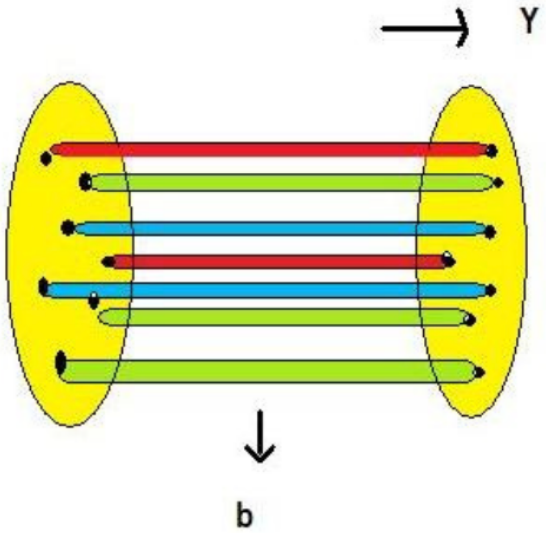

$S_1 = \pi r_0^2$

$r_0 \sim 0.25$ fm

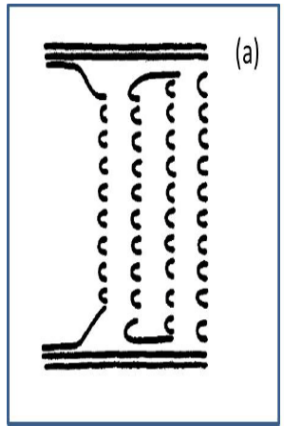

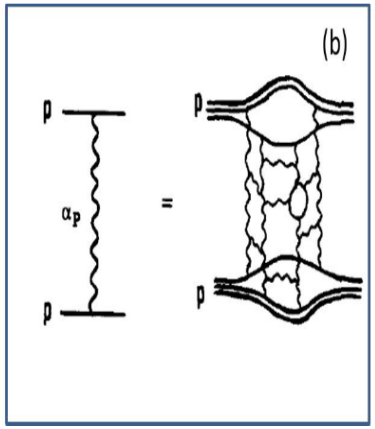

Multi particle production at high energies is currently described in terms of color strings stretched between the projectile and target.
These strings decay into new ones by production and subsequently hadronize to produce the observed hadrons.

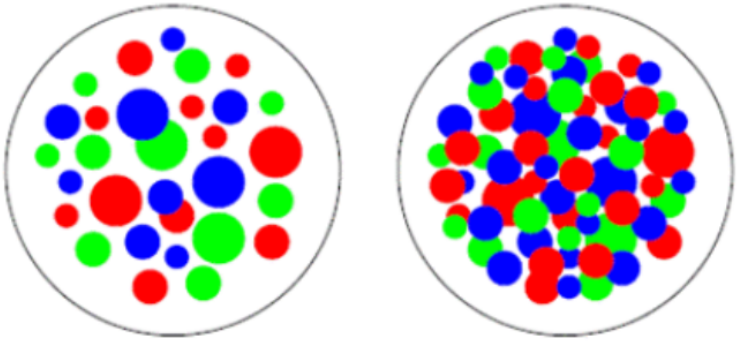

De-confinement is expected when the density of quarks and gluons becomes so high that would overlap strongly.

We have clusters within which color is not longer confined : De-confinement is thus related to cluster formation very much similar to cluster formation in percolation theory and hence a connection between percolation and de-confinement seems very likely.

Parton String Percolation Model

- At a critical density, a macroscopic cluster appears and mark a geometric phase transition.

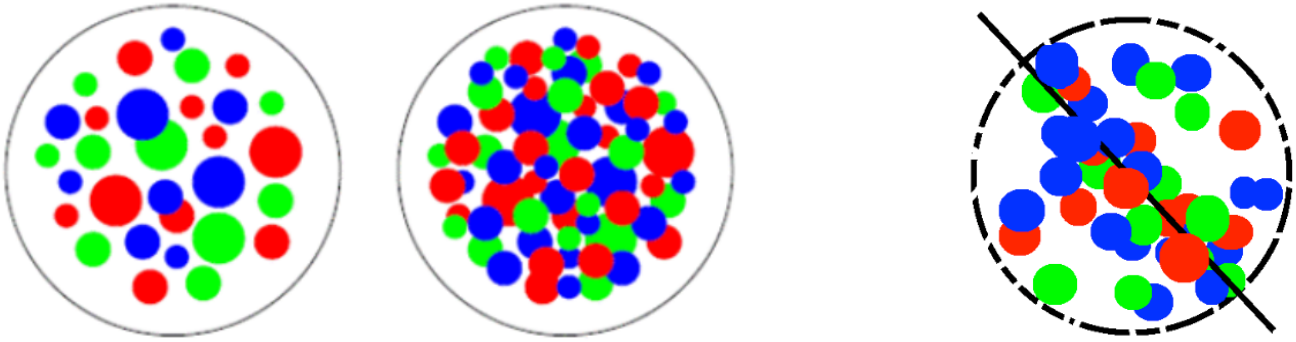

- Due to the random sum of the color charges in SU(3) the total charge decrease the particle multiplicity and gives an increase on the average tension of the strings
- A cluster of n strings that occupies an area Sn behaves as a single color source with a higher color field corresponding to a vectorial sum of color charges of each individual string

$$\vec{Q}_n^{\,2} = n\vec{Q}_1^{\,2} \longrightarrow \text{If strings are fully overlap}$$

$$\vec{Q}_n^{\,2} = n\frac{S_n}{S_1}\vec{Q}_1^{\,2} \longrightarrow \text{Partially overlap}$$

- The extended string between partons decays to new pairs of strings that latter form new partons which eventually hadronize (fragmentation). The particles are produce by the parton interactions via the Schwinger mechanism

Multiplicity and $\langle p_T^2 \rangle$ of particles produced by a cluster of n strings

multiplicity → $\frac{dn}{dy} \sim F(\xi)\bar{N}_s$

color reduction factor → $F(\xi) = \sqrt{\frac{1-e^{-\xi}}{\xi}}$

Number of strings → $N_p^s = 2 + 4\left(\frac{r_0}{R_p}\right)^2 \left(\frac{\sqrt{s}}{m_p}\right)^{2\lambda}$

string density in pp collisions → $\xi = N_p^s \left(\frac{r_0}{R_p}\right)^2$

$\lambda = .201$

proton mass

proton radius

M. A. Braun and C. Pajares, Eur. Phys. J. C16,349 (2000)
M. A. Braun et al, Phys. Rev. C65, 024907 (2002)

- The critical parameter is the string density

$$\xi = N_s \frac{S_1}{S_A},\ \xi_c = 1.1 - 1.5$$

- The area cover when one reach the critical densit $1 - e^{-\xi}$

- We assume that the cluster behaves like a single string but with higher color field and momentum

- In the large (n) limit the multiplicities and momentum sums:

$$< \mu_n >= \sqrt{\frac{nS_n}{S_1}} < \mu_1 > \ , < p_{Tn}^2 >= \sqrt{\frac{nS_1}{S_n}} < p_{T1}^2 >$$

Similar scaling laws are obtained for the product and the ratio of the multiplicities and transverse momentum in CGC

Both provide explanation for multiplicity suppression and $<p_T>$ scaling with dN/dy.

Momentum Qs establishes the scale in CGC with the corresponding one in percolation of strings

The no. of color flux tubes in CGC and the effective no. of clusters of strings in percolation have the same dependence on the energy and centrality. (implications in Long range rapidity correlations and the ridge structure).

Clustering strings ~gluon saturation

$$Q_s^2 = \frac{k\langle p_T^2\rangle_1}{F(\xi)}$$

$$Q_s^2 \sim \sqrt{(\xi)}$$

Y. V. Kovchegov, E. Levin, L. McLerran, Phys. Rev. C 63, 024903 (2001).
I. Bautista, J. Dias de Deus, C. Pajares, AIP Conf.Proc. 1343 (2011) 495-497

1. Multiplicity
2. p_T distribution
3. Particle ratios
4. Elliptic flow
5. Suppression of high pt particles RAA
6. J/ψ production
7. Forward -Backward Multiplicity Correlations at RHIC and LHC

Braun, Dias de Deus, Hirsch, Pajares, Scharenberg and Srivastava Phys. Rep. 599 (2015)

Properties of Small collision systems
QGP Droplet

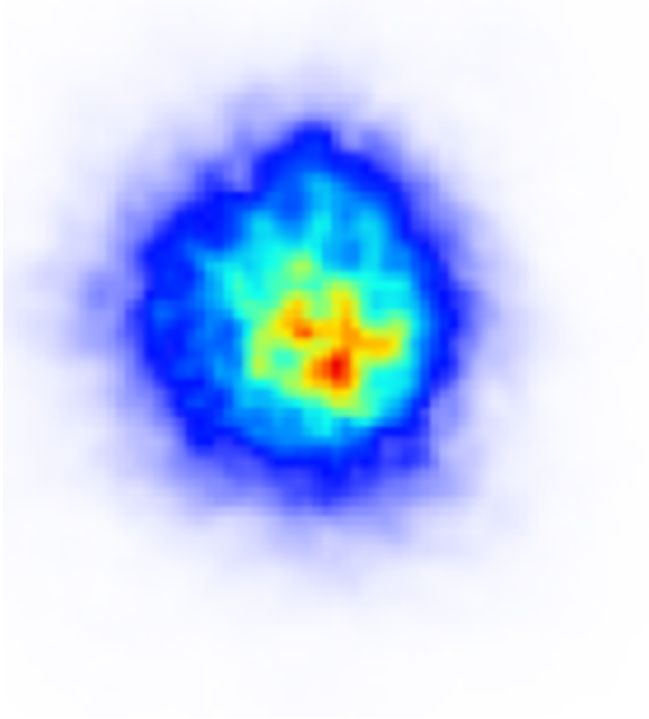

Thermodynamics on SPM

The model allows to relate concepts like temperature, entropy, and viscosity among other quantities as a function of the parameters

$$\zeta^t \,\&\, F(\zeta^t)$$

The Schwinger mechanism for no massive particles is given by:

$$\frac{dN}{dp_T} \sim e^{-\sqrt{2F(\zeta^t)}\frac{p_T}{\langle p_T\rangle_1}}$$

which can be related with the average value of the string tension of the strings $\langle x^2\rangle = \pi\langle p_T^2\rangle_1/F(\zeta)$ These value fluctuates around its mean value since the chromo electric filed is not constant, and the fluctuations gives a Gaussian distribution of the string tension which can be seen as a thermal distribution.

$$T(\zeta^t) = \sqrt{\frac{\langle p_T^2\rangle_1}{2F(\zeta^t)}}$$

H. G. Dosch, Phys. Lett. 190 (1987) 177 A. Bialas, Phys. Lett. B 466 (1999) 301

Power law for the transverse momentum distribution

$$\frac{d^2N}{dp_T^2} = \omega(\alpha, p_0, p_T) = \frac{(\alpha-1)(\alpha-2)}{2\pi p_0^2} \frac{p_0^\alpha}{[p_0+p_T]^\alpha}$$

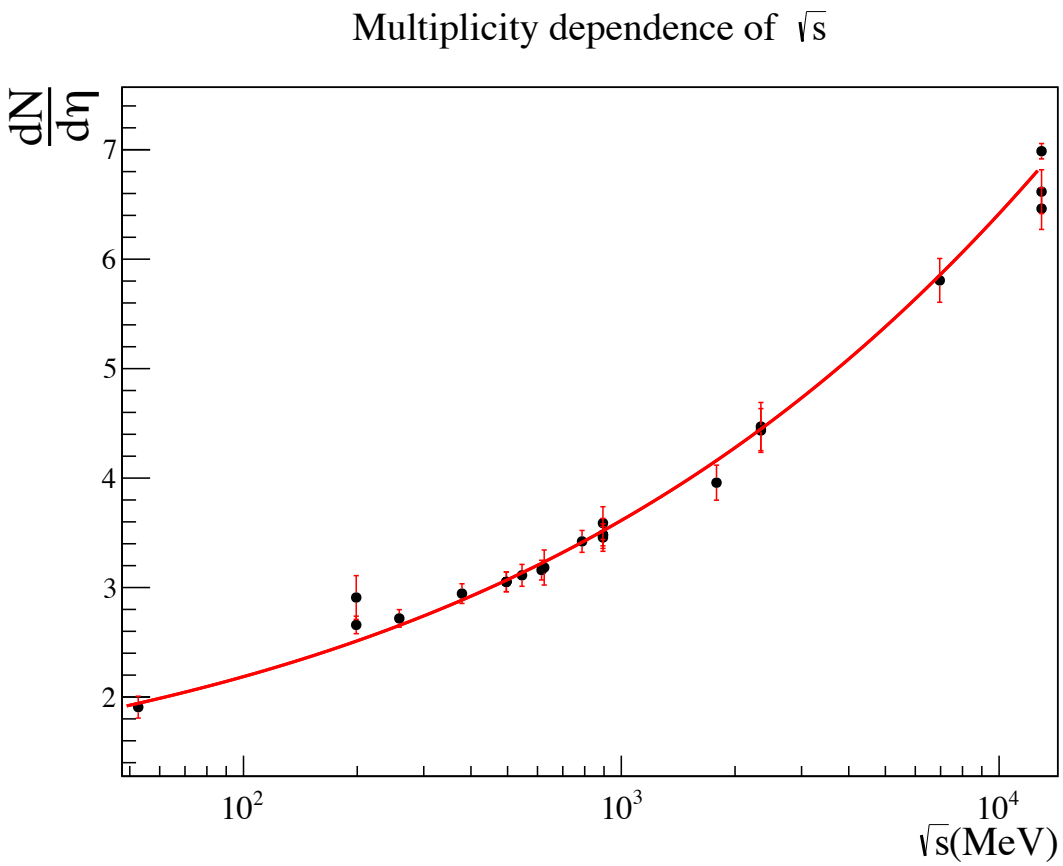

Nucl. Phys. A 698, 331 (2002)

I. Bautista, C. Pajares, J. G. Milhano and J. Dias de Deus, Phys. Rev. C **86** (2012) 034909

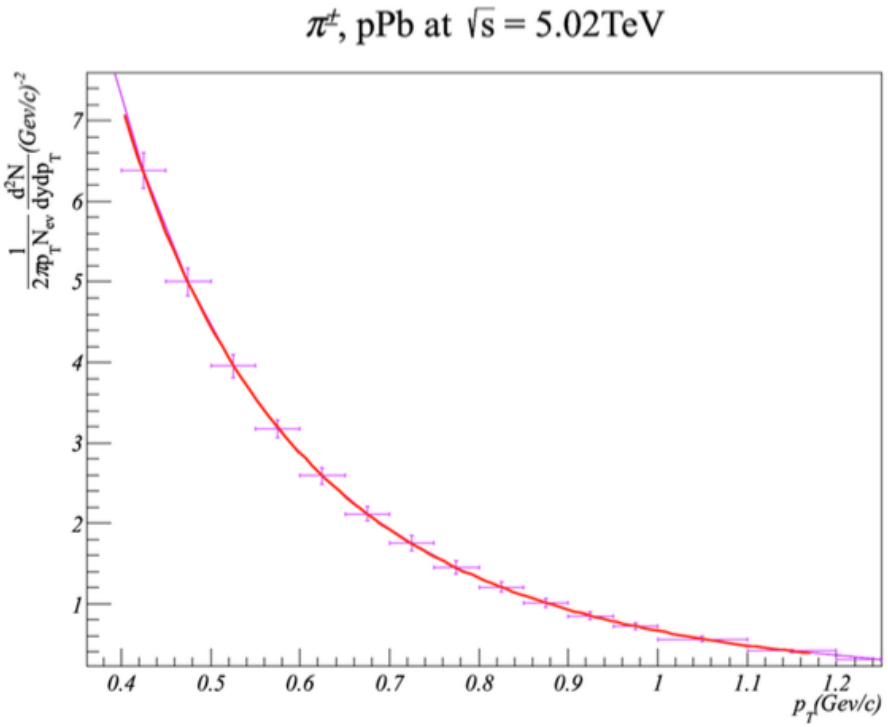

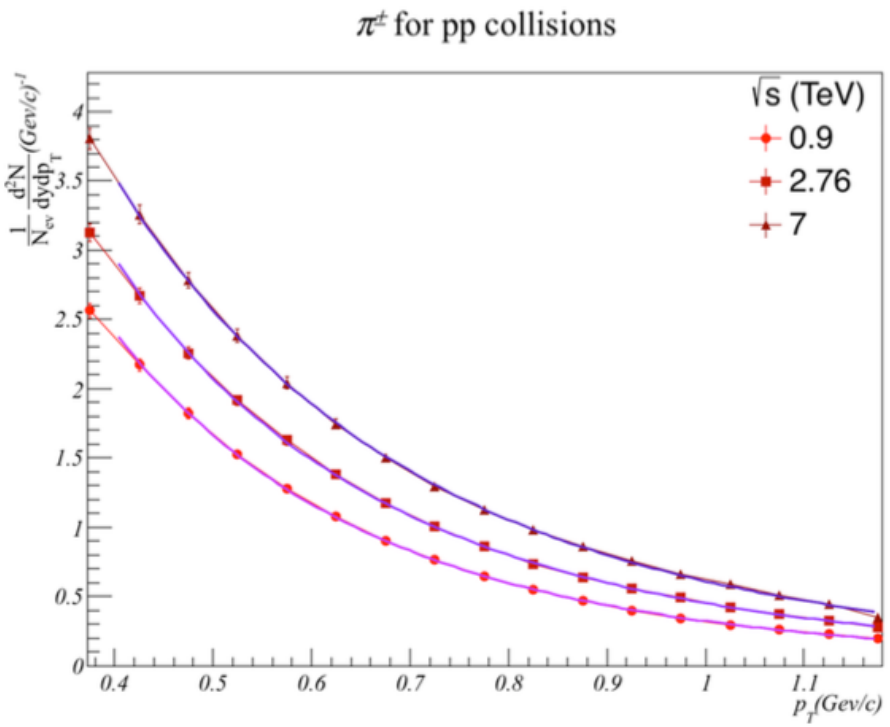

$\sqrt{S}(TeV)$	a	p_0	α
5.02	29.63±67.6	3.35±9.14	10.83±22.02
7	33.48±9.3	2.32±0.88	9.78±2.53
2.76	22.48±4.2	1.54±0.46	7.94±1.41
0.9	23.29±4.48	1.82±0.54	9.4±1.8

B. B. Abelev *et al.* [ALICE Collaboration], Eur. Phys. J. C **74** (2014) no.9, 3054

S. Chatrchyan *et al.* [CMS Collabora- tion], Eur. Phys. J. C **72**, 2164 (2012)

Power law for the transverse momentum distribution

$$\frac{d^2N}{dp_T^2} = \omega(\alpha, p_0, p_T) = \frac{(\alpha-1)(\alpha-2)}{2\pi p_0^2} \frac{p_0^\alpha}{[p_0+p_T]^\alpha}$$

$$\frac{d^2N}{dp_T^2} = \frac{(\alpha-1)(\alpha-2)(p_0\sqrt{\frac{F(\zeta_{pp})}{F(\zeta_{HM})}})^{\alpha-2}}{2\pi[p_0\sqrt{\frac{F(\zeta_{pp})}{F(\zeta_{HM})}}+p_T]^\alpha}$$

$$\frac{1}{N}\frac{d^2N}{d\eta dp_T} = a'(\sqrt{s})\frac{dN}{d\eta}\Big|^{pp}_{\eta=0}(\sqrt{s})\omega(\alpha, p_0, p_T) = \frac{a(p_0\frac{F(\zeta_{pp})}{F(\zeta_{HM})})^{\alpha-2}}{[p_0\sqrt{\frac{F(\zeta_{pp})}{F(\zeta_{HM})}}+p_T]^{\alpha-1}}$$

Nucl. Phys. A 698, 331 (2002)

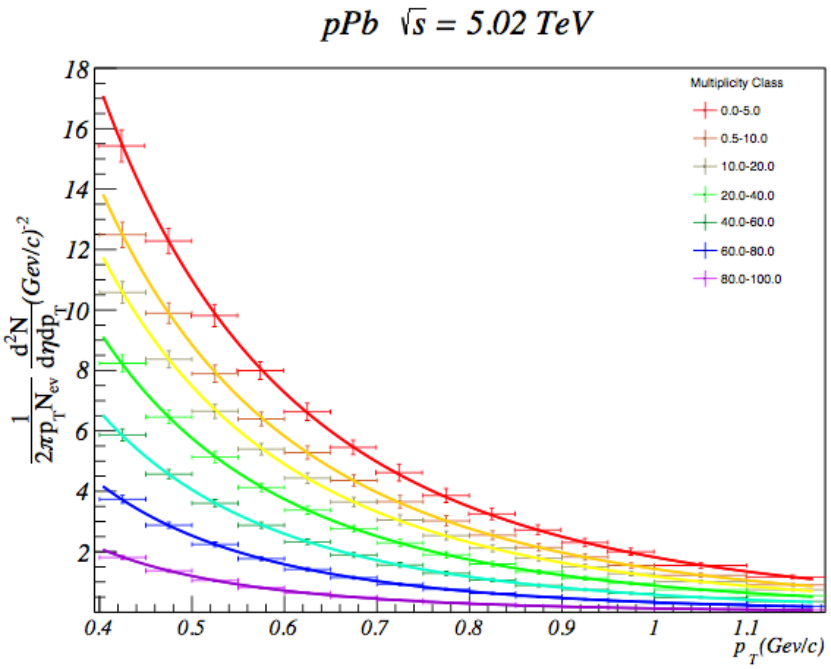

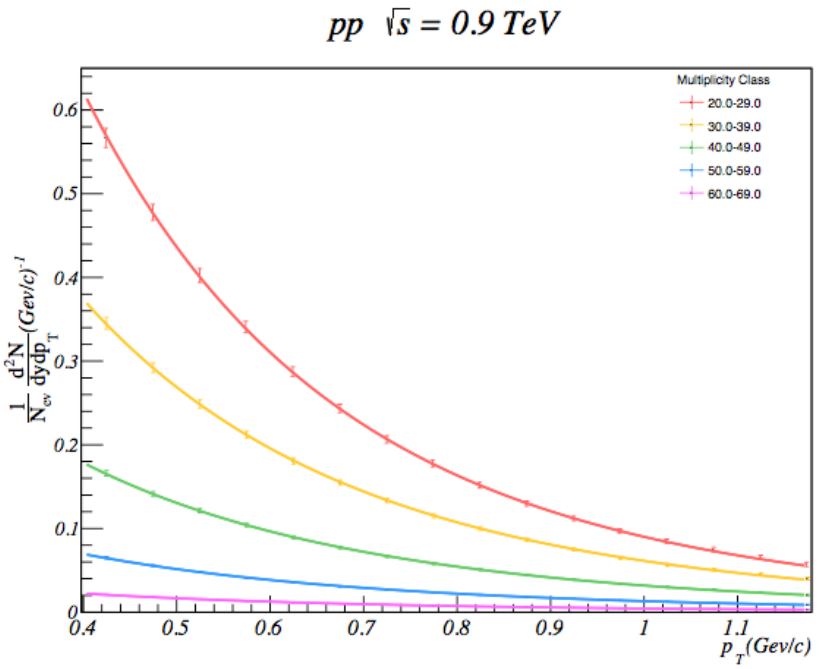

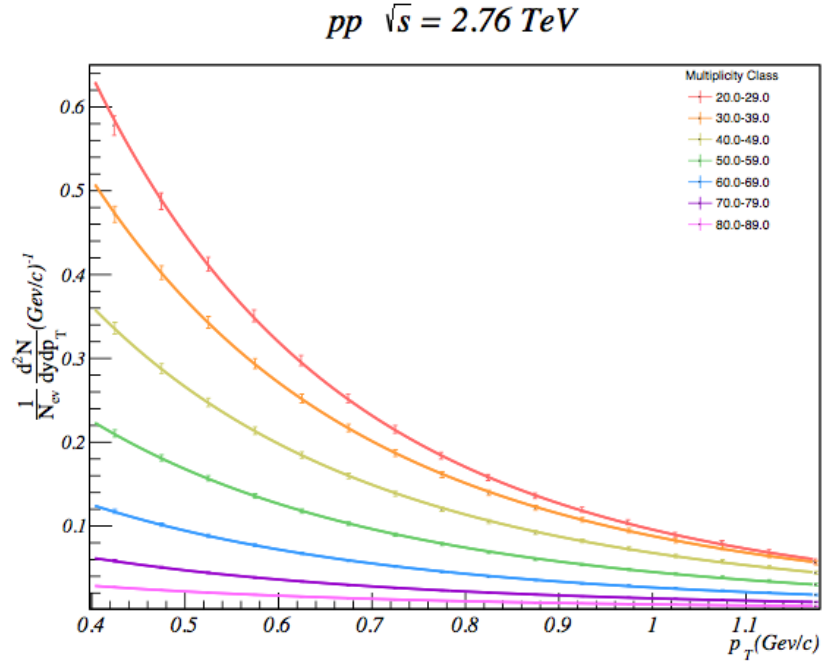

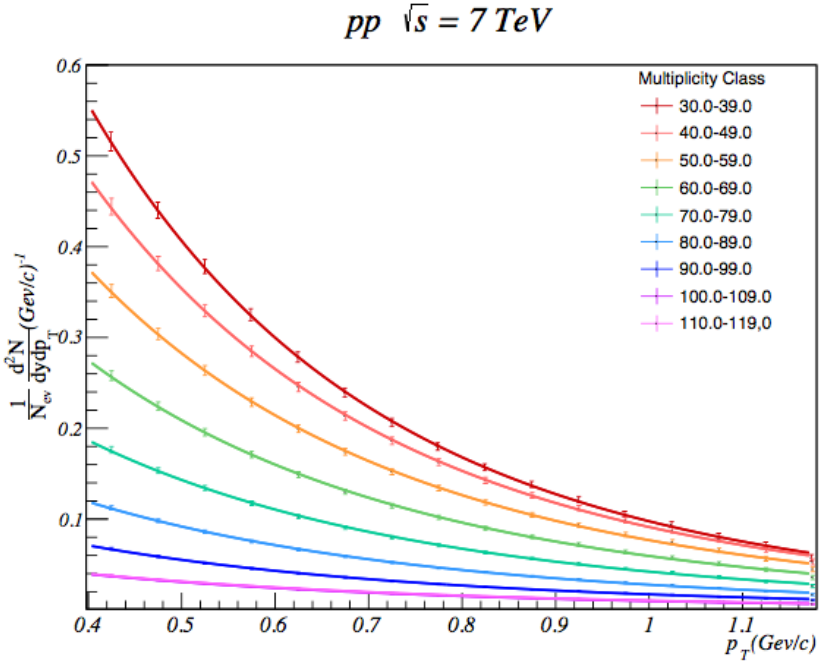

B. B. Abelev *et al.* [ALICE Collaboration], Eur. Phys. J. C **74** (2014) no.9, 3054

S. Chatrchyan *et al.* [CMS Collabora- tion], Eur. Phys. J. C **72**, 2164 (2012)

Color reduction factor

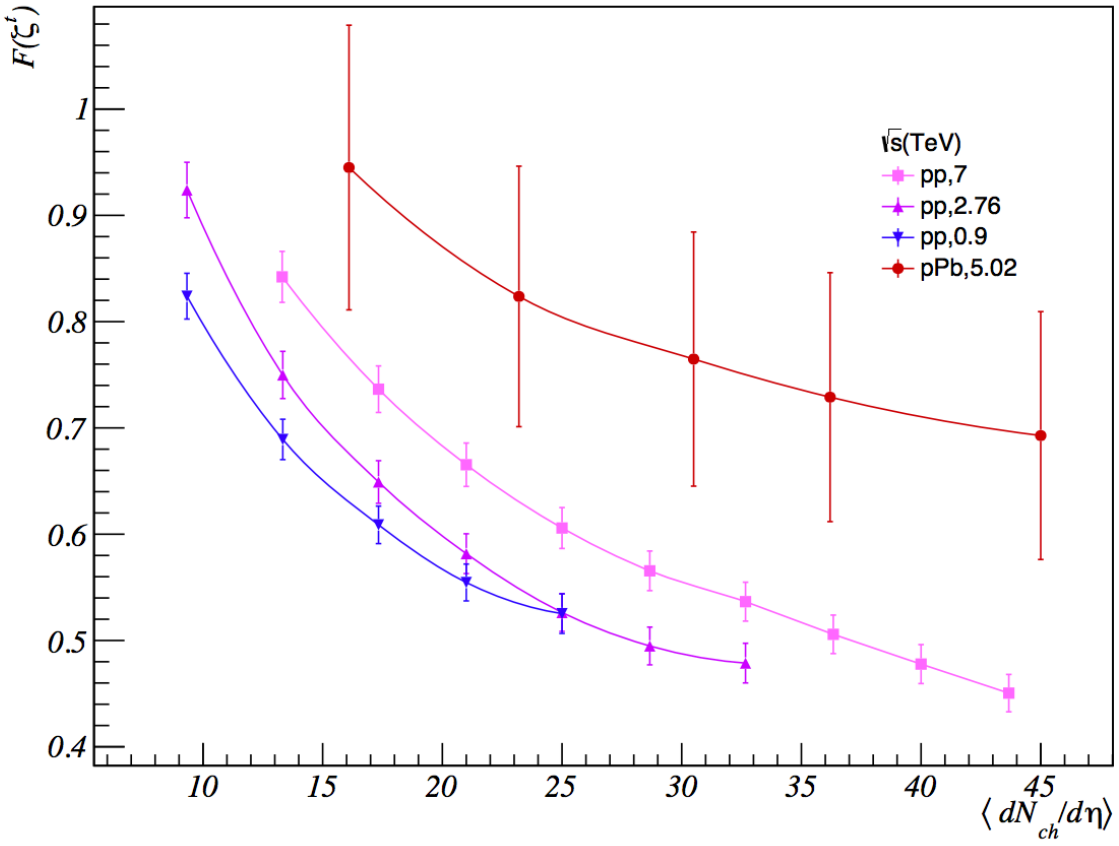

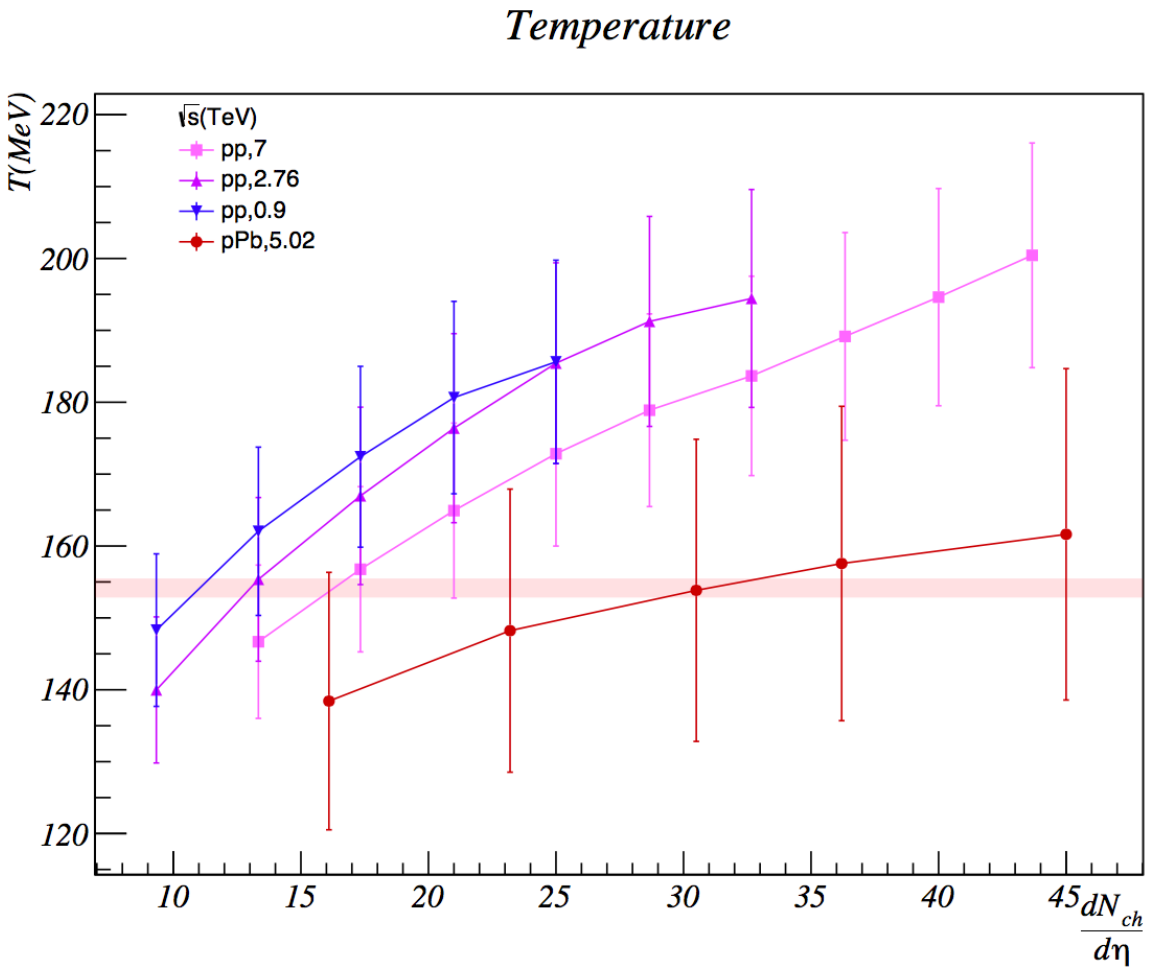
Temperature
T(MeV)
220
200
180
160
140
120
√s(TeV)
pp,7
pp,2.76
pp,0.9
pPb,5.02
10
15
20
25
30
35
40
45
dN_ch/dη

To fit data we use the scaling $1-e^{p(\mu)}$, where $p(\mu)$ is a polynomial in multiplicity considering a limit for very high multiplicities F_0 is the limit on saturation scale and we have a logarithmic dependence on the ratio of the energy over the threshold $\sim 1/\ln(s_0/s)$ of gluon saturation 2

$$F(\zeta^t) = F_0 + \frac{1 - \exp\left[\left(\frac{\mu}{\mu_0} + a_1\right)^{\frac{\sqrt{s}}{\sqrt{s_0}}}\right]}{a_0 \ln\left(\frac{\sqrt{s_0}}{\sqrt{s}}\right)}, \quad (1)$$

Fit over diferent classes of multiplicity

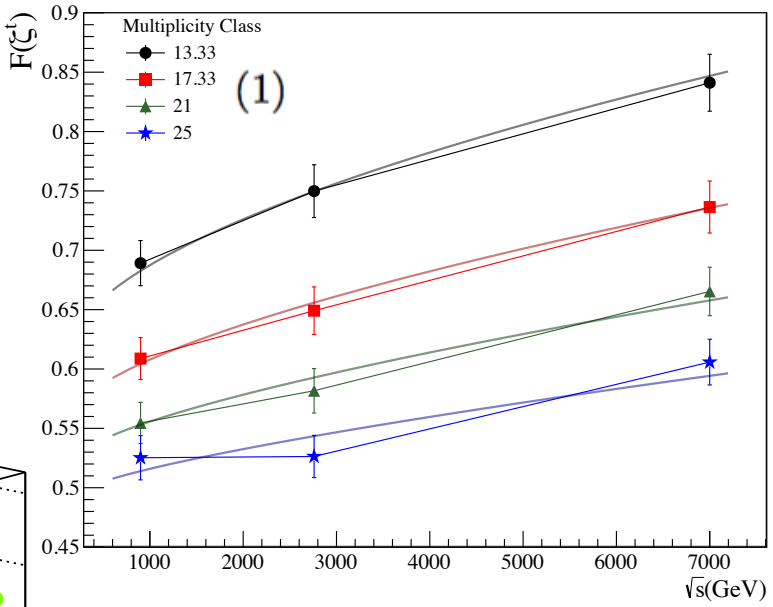

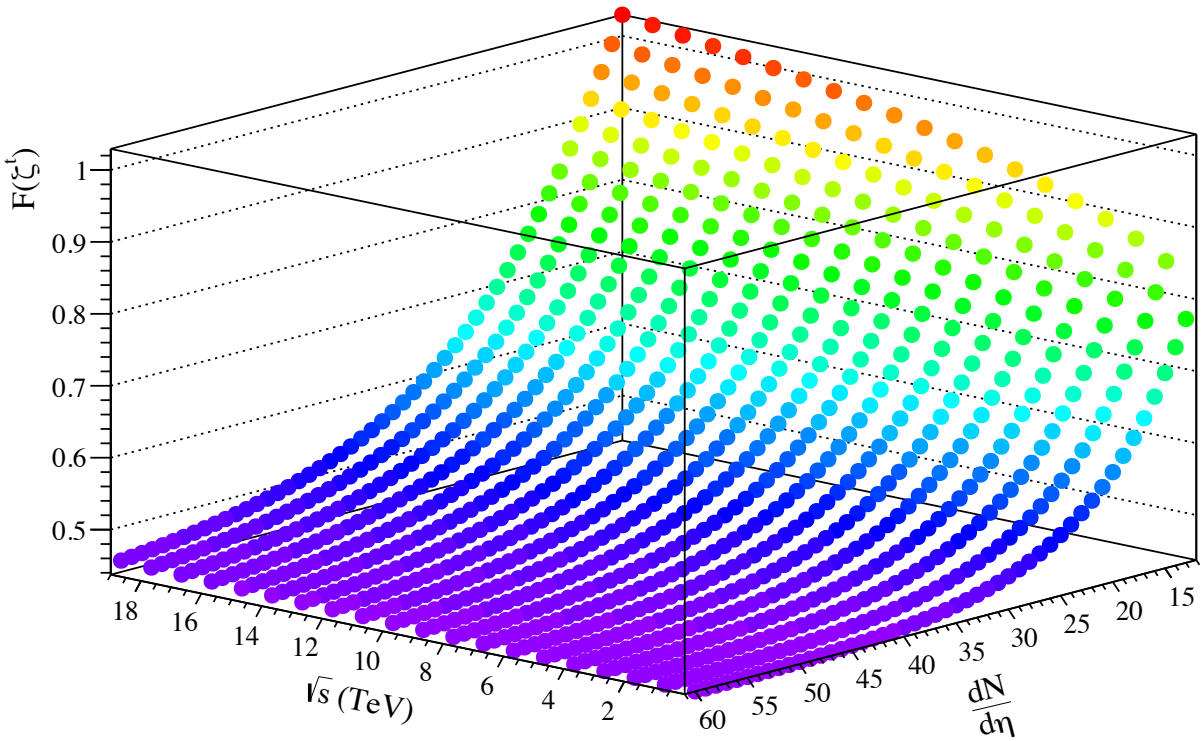

parameter	value	error
F_0	0.435241	0.0503243
$\sqrt{s_0}(\times 10^3 \text{TeV})$	1.40030	1.49161
μ_0	54.468	16.2556
a_1	0.00258187	0.00470024
a_0	0.119777262	0.026209073
a_0^{-1}	8.34883	1.82685

Monte Carlo

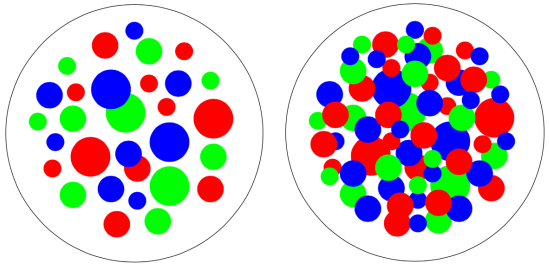

$$\varepsilon = \sqrt{1 - \frac{b^2}{a^2}}$$

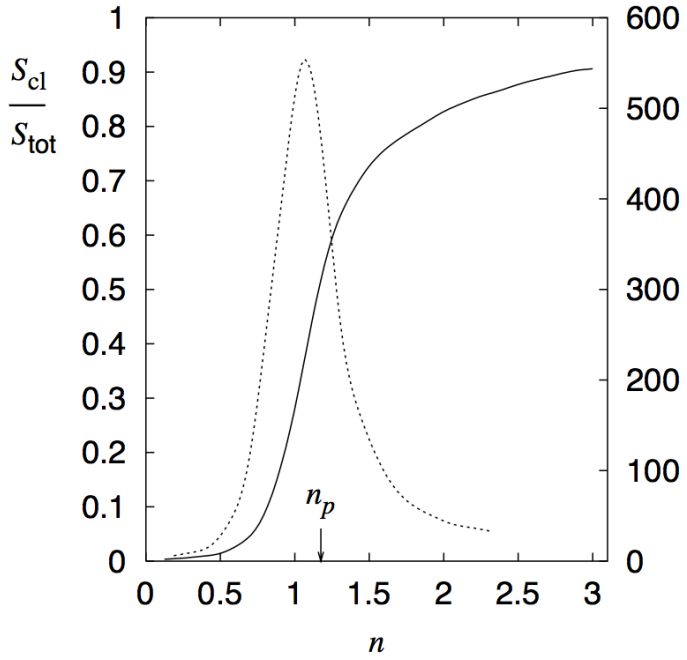

$$\eta = \frac{r_0^2 N}{ab}. \qquad a^2 = \frac{r_0^2 N}{\eta\sqrt{1-\varepsilon^2}}; \qquad b^2 = \frac{r_0^2 N\sqrt{1-\varepsilon^2}}{\eta}$$

Once determined a and b, we take a random point (x, y) distributed in the rectangle $[-(a - r_0), a - r_0] \times [-(b - r_0), b - r_0]$ according with a density profile. This point is the center of the string and it is included in the string population if satisfies the following condition

$$\frac{x^2}{(a - r_0)^2} + \frac{y^2}{(b - r_0)^2} \leq 1.$$

The constrictions will only consider strings completely embedded in the elliptical region. In this way, we can generate all N strings needed to build the percolating system. Note that with this construction, in the limit $\varepsilon = 0$, we recover the particular case for a SPM bounded by circles, which has been already studied by several authors

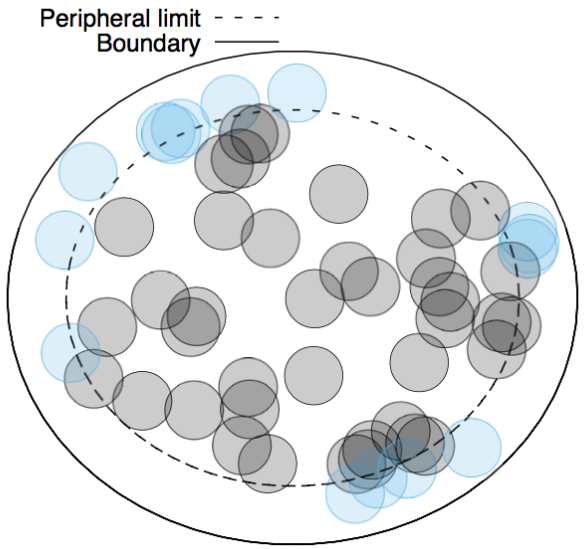

The solid line is the elliptic boundary of the system and the dashed line represents the internal peripheral limit needed to define a spanning cluster. Blue circles are the peripheral strings satisfying the relation

$$\frac{x^2}{(a-2r_0)^2} + \frac{y^2}{(b-2r_0)^2} > 1.$$

In this way, we assure that there is a spanning cluster in the string system if the largest cluster has more than one peripheral string and the largest distance between the peripheral strings is greater than $2(b - 2r_0)$. This ensure that the spanning cluster at least cross-over the system through the minor semi-axes.

Density Profiles

$$f(x,y) = \frac{1}{2\pi\sigma_a\sigma_b}\exp\left[-\frac{1}{2}\left(\frac{x^2}{\sigma_a^2}+\frac{y^2}{\sigma_b^2}\right)\right]:$$

$$\sigma_a = (a-r_0), \quad \sigma_b = (b-r_0);$$
$$\sigma_a = (a-r_0)/2^{1/2}, \quad \sigma_b = (b-r_0)/2^{1/2};$$
$$\sigma_a = (a-r_0)/2, \quad \sigma_b = (b-r_0)/2.$$

σ_a and σ_b are standard deviations over the semi-axis of the ellipse

$1s$, $2^{1/2}s$ y $2s$

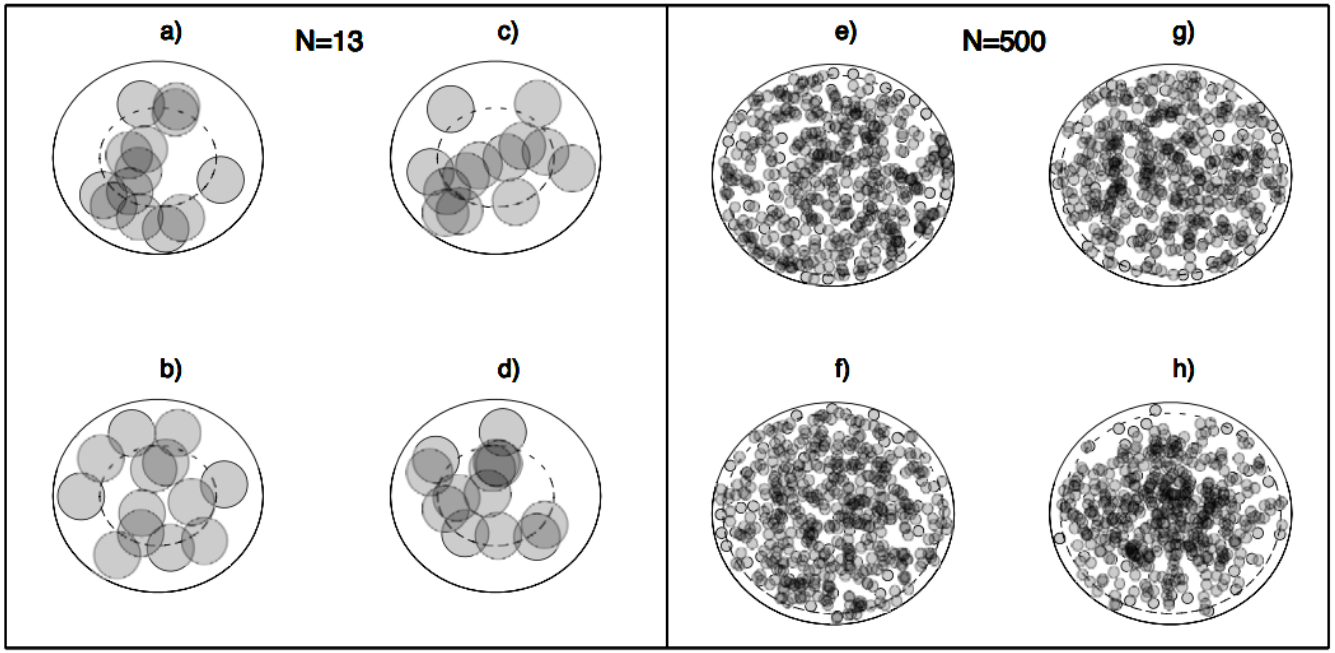

Samples of a percolating system for different density profiles. Left box: String systems at $N = 13$, $\eta = 0.7$ and $\varepsilon = 0.4$, for the models a) Uniform, b) $1s$, c) $2^{1/2}s$ and d) $2s$; Right box: String systems at $N = 500$, $\eta = 1.1$ and $\varepsilon = 0.4$, for the models e) Uniform, f) $1s$, g) $2^{1/2}s$ and h) $2s$.

String percolation threshold for elliptically bounded systems, I. Bautista, A. Fernández. J. E Ramirez, Physica 488 (2017) 8-15.

Among profiles there is not much differences but we expect to have larger differences as we increase the number of strings.

As the number of peripheral discs decrease the percolation threshold becomes higher

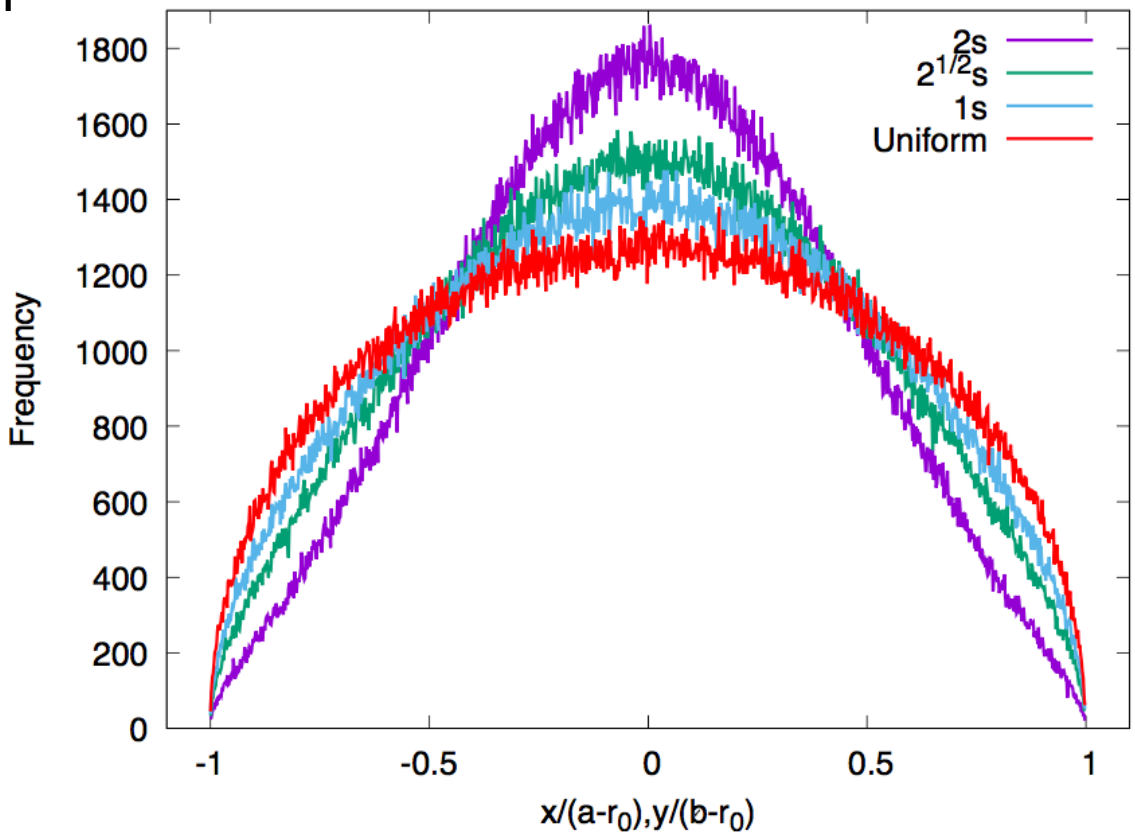

Projection of the disc position distribution over the axis of the ellipse for the different profile functions. The histograms were built with a 10^6 generated positions for each model. The distributions are normalized to the semi-axis value to eliminate the dependence on the number of discs N, ε and η.

String percolation threshold for elliptically bounded systems, I. Bautista, A. Fernández. J. E Ramirez, Physica 488 (2017) 8-15.

The percolation threshold appears when the derivative ∂P/∂η takes its maximum value

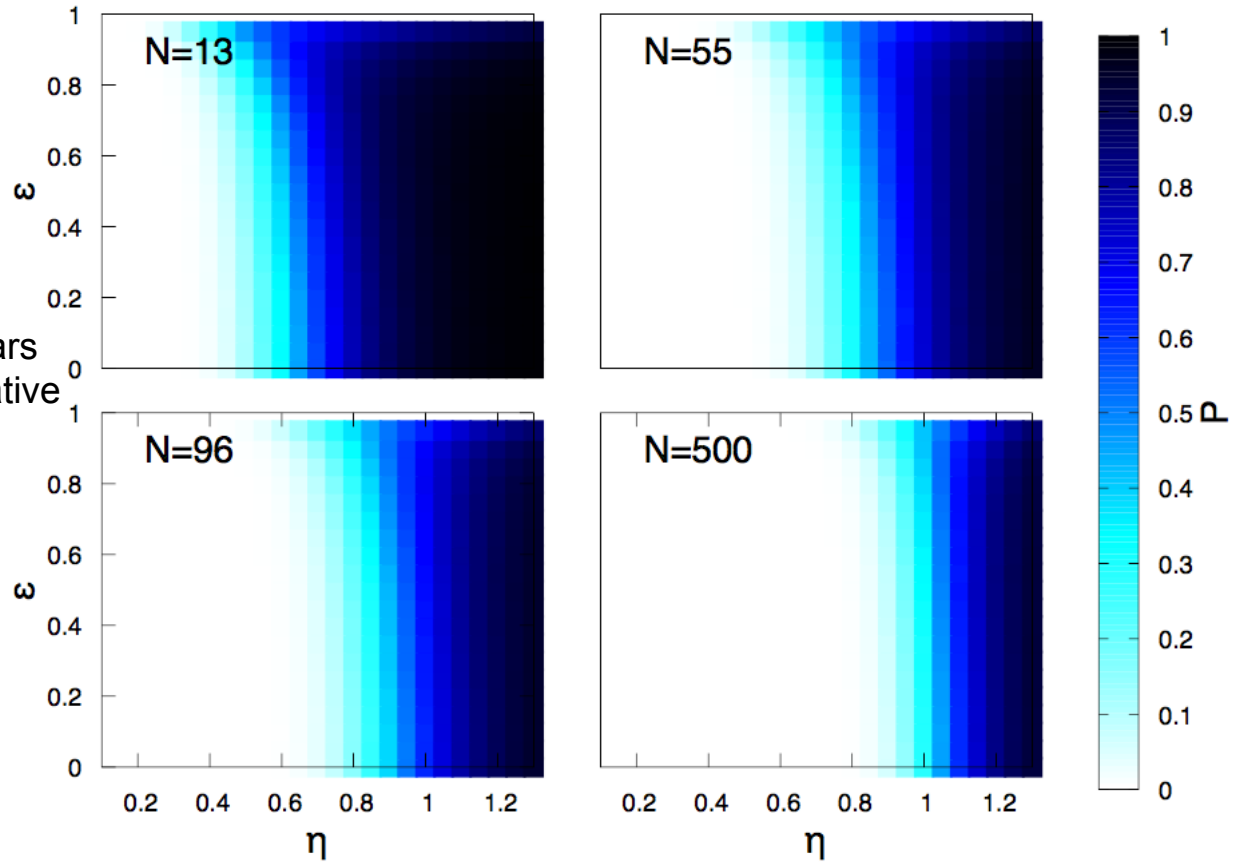

The percolation probability shows an evident shift as a function of N and high eccentricity dependence associated with a finite size effect.

Percolation probability P as a function of filling factor η and eccentricity ε for different values of a number of strings N with Uniform density profile.

For largest values of N, the percolation probability becomes independent of the eccentricity and the phase transition appears around the percolation threshold for the continuum percolation in the thermodynamic limit.

String percolation threshold for elliptically bounded systems, I. Bautista, A. Fernández. J. E Ramirez, Physica 488 (2017) 8-15.

$$P(\eta) = \frac{1}{1 + \exp\left(-\sum_{k=0}^{4} a_k \eta^k\right)}$$

the fraction of occupied/connected sites belonging to the spanning cluster

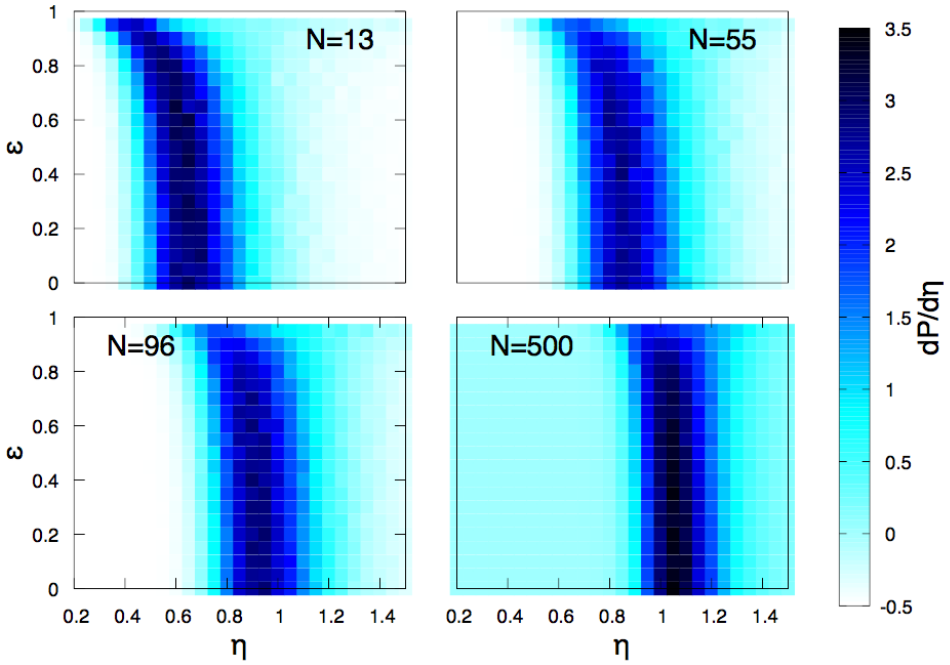

A derivative of the percolation probability with respect to filling factor η in the Uniform model.

To obtain the value of η_c, the equation $P(\eta_c) = 0.5$ has to be solved. However, for N = 500 and the model with Gaussian density profiles, we use

$$P(\eta) = \frac{1}{2}\left[1 + \tanh\left(\frac{\eta - \eta_c}{\Delta L}\right)\right]$$

where η_c is the percolation threshold and ΔL is the width of the percolation transition. In Fig. 7, we show the best fit obtained for the percolation probability as a function of filling factor for different values of η and N in string percolating systems with Uniform density profile

String percolation threshold for elliptically bounded systems, I. Bautista, A. Fernández. J. E Ramirez, Physica 488 (2017) 8-15.

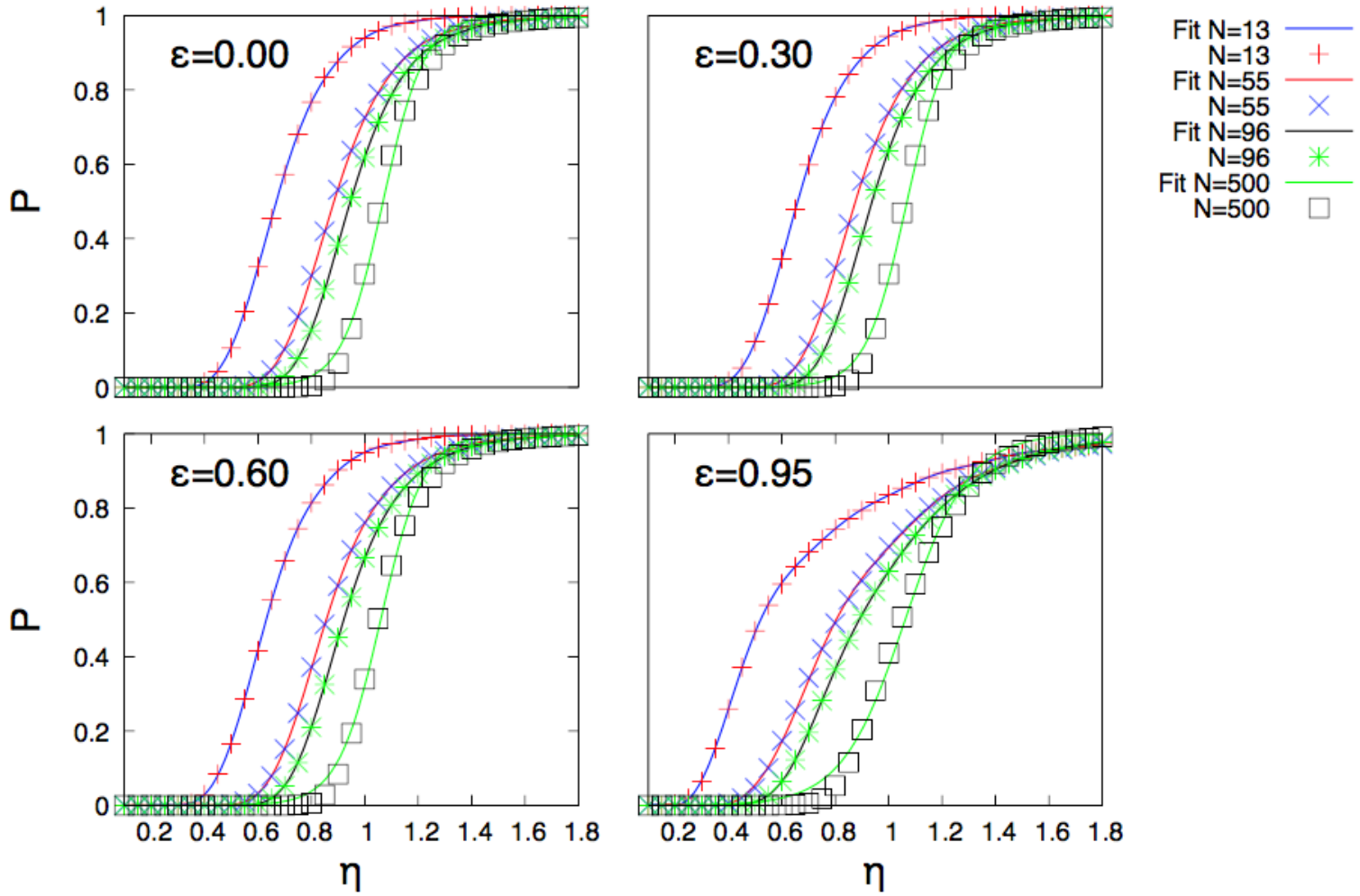

String percolation threshold for elliptically bounded systems, I. Bautista, A. Fernández. J. E Ramirez, Physica 488 (2017) 8-15.

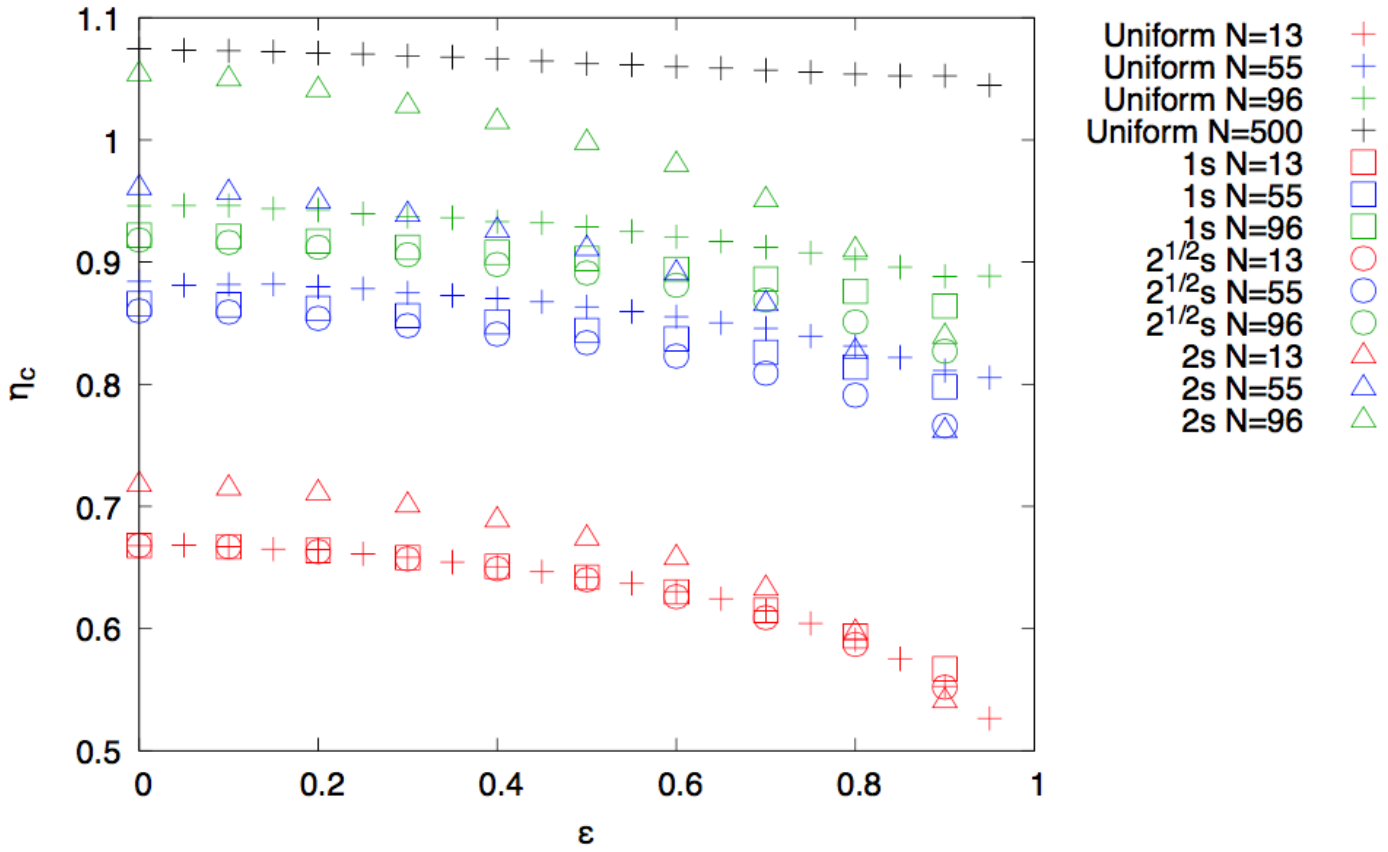

Percolation threshold η_c as a function of eccentricity (ε) for different values of N with the different density profiles: Uniform (crosses), and Gaussian: $1s$ (squares), $2^{1/2}s$ (circles) and $2s$ (triangles).

String percolation threshold for elliptically bounded systems, I. Bautista, A. Fernández. J. E Ramirez, Physica 488 (2017) 8-15.

How far from the thermodynamic limit?

$$\frac{\eta}{1-\exp(-\eta)} \equiv \frac{1}{F^2(\eta)} \longrightarrow \mu = N_S F(\eta)\mu_1 \; ; \; \langle p_{\rm T}^2 \rangle = \langle p_{\rm T}^2 \rangle_1 / F(\eta)$$

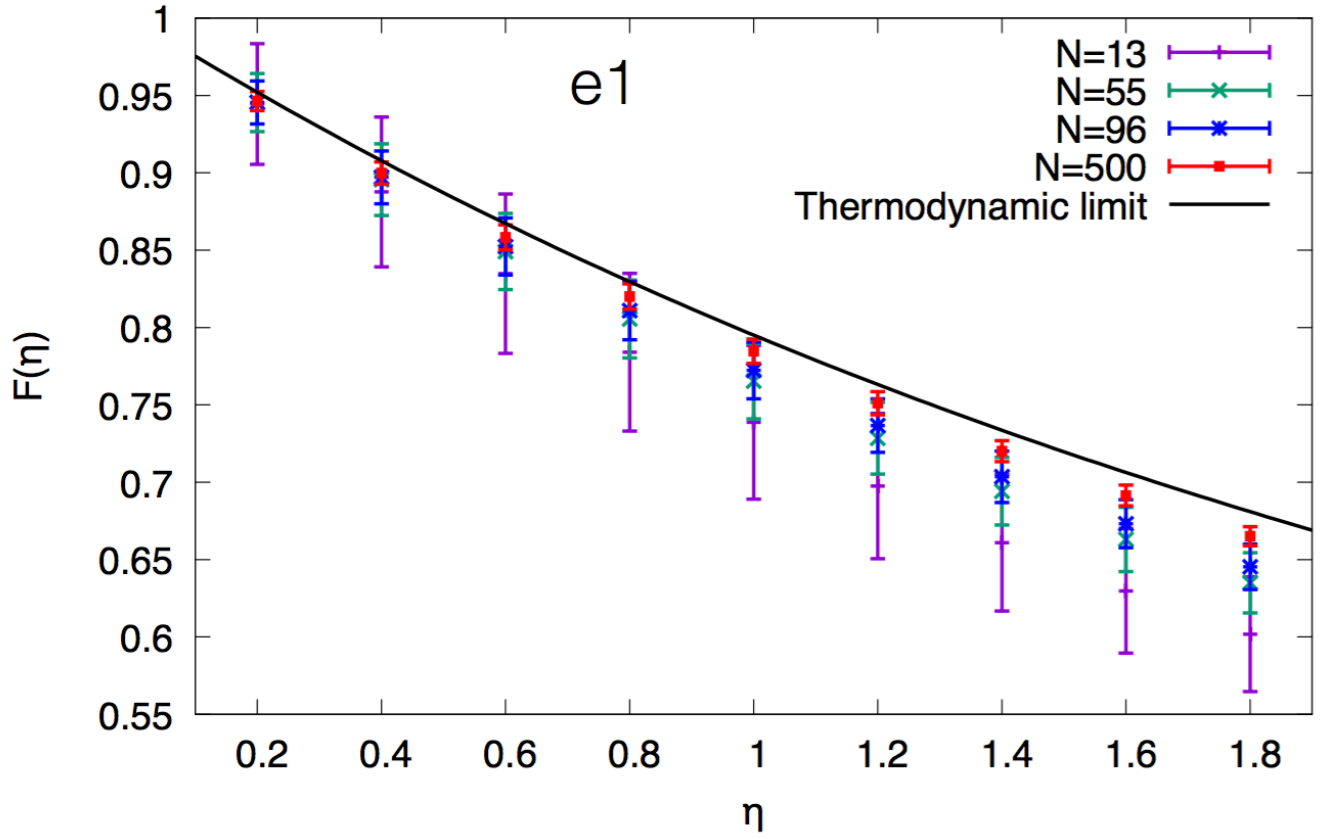

Initial geometry fluctuations of the droplet?

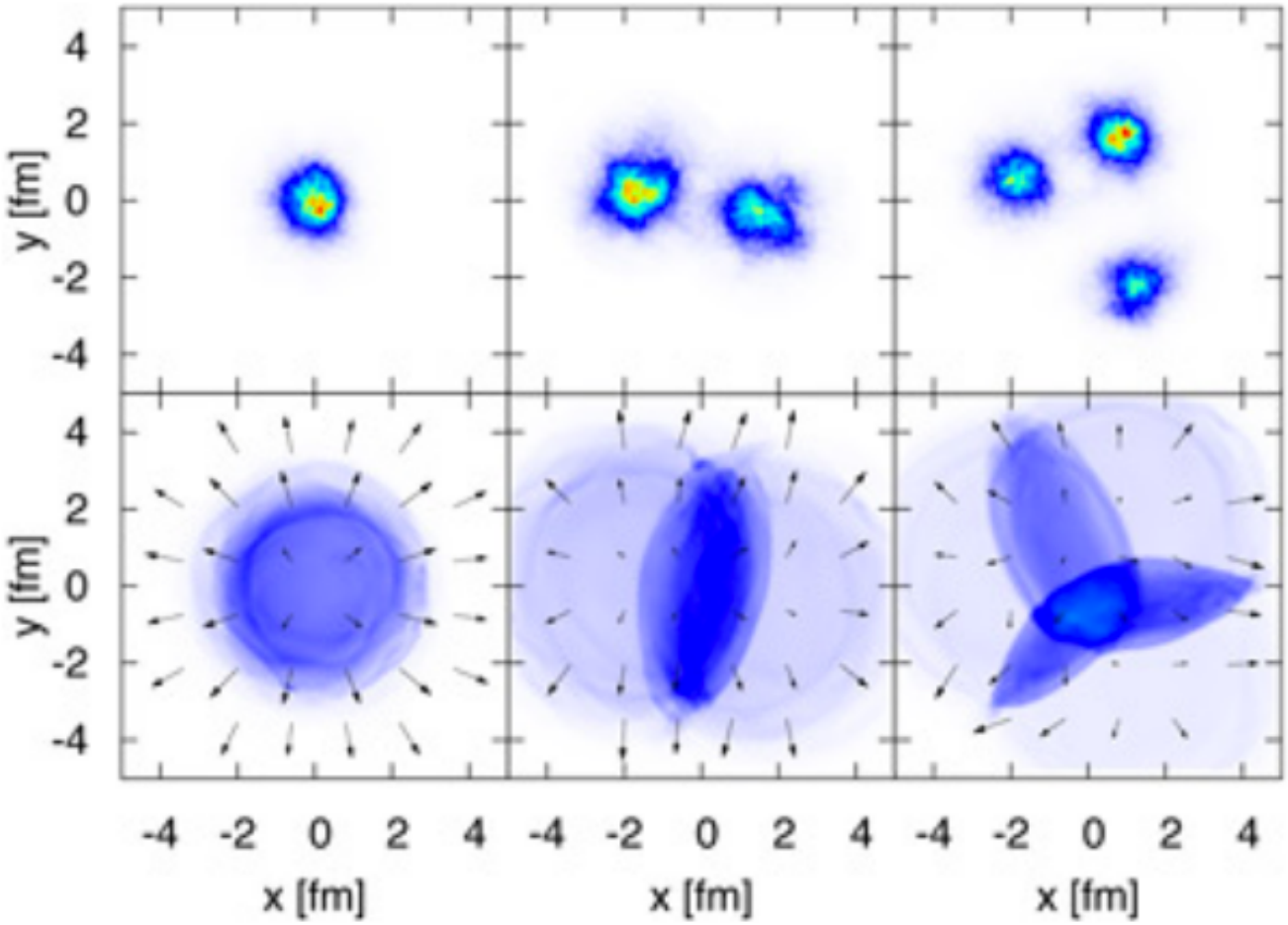

Image taken from Bjoern Schenke The Drops of Early Universe Perfect Fluid, Brookhaven Newsroom

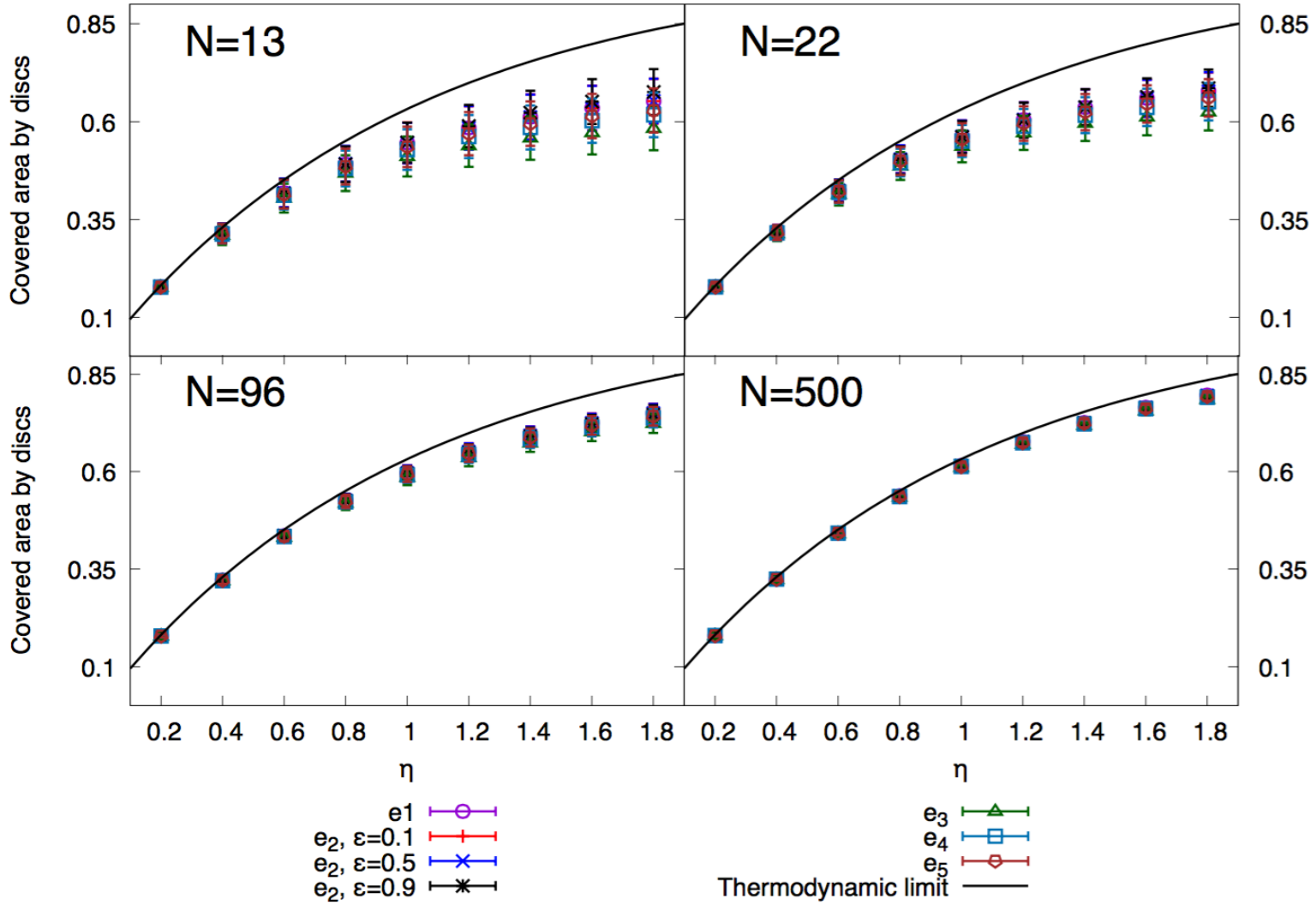
N=13
N=22
N=96
N=500
Covered area by discs
Covered area by discs
0.85
0.6
0.35
0.1
0.2
0.4
0.6
0.8
1
1.2
1.4
1.6
1.8
η
η
e1
e2, ε=0.1
e2, ε=0.5
e2, ε=0.9
e3
e4
e5
Thermodynamic limit

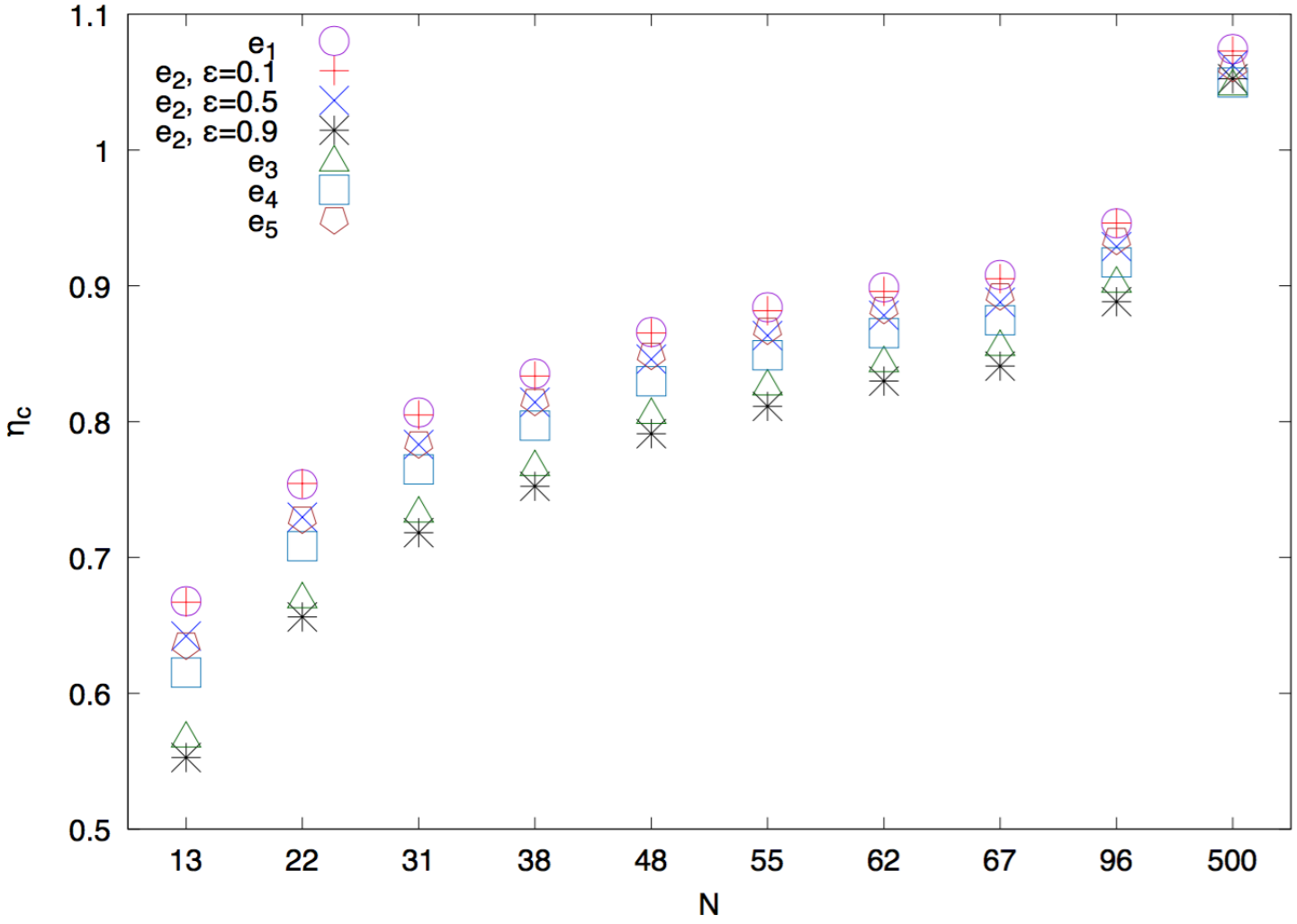
1.1
1
0.9
0.8
0.7
0.6
0.5
η_c
13
22
31
38
48
55
62
67
96
500
N
e_1
e_2, ε=0.1
e_2, ε=0.5
e_2, ε=0.9
e_3
e_4
e_5

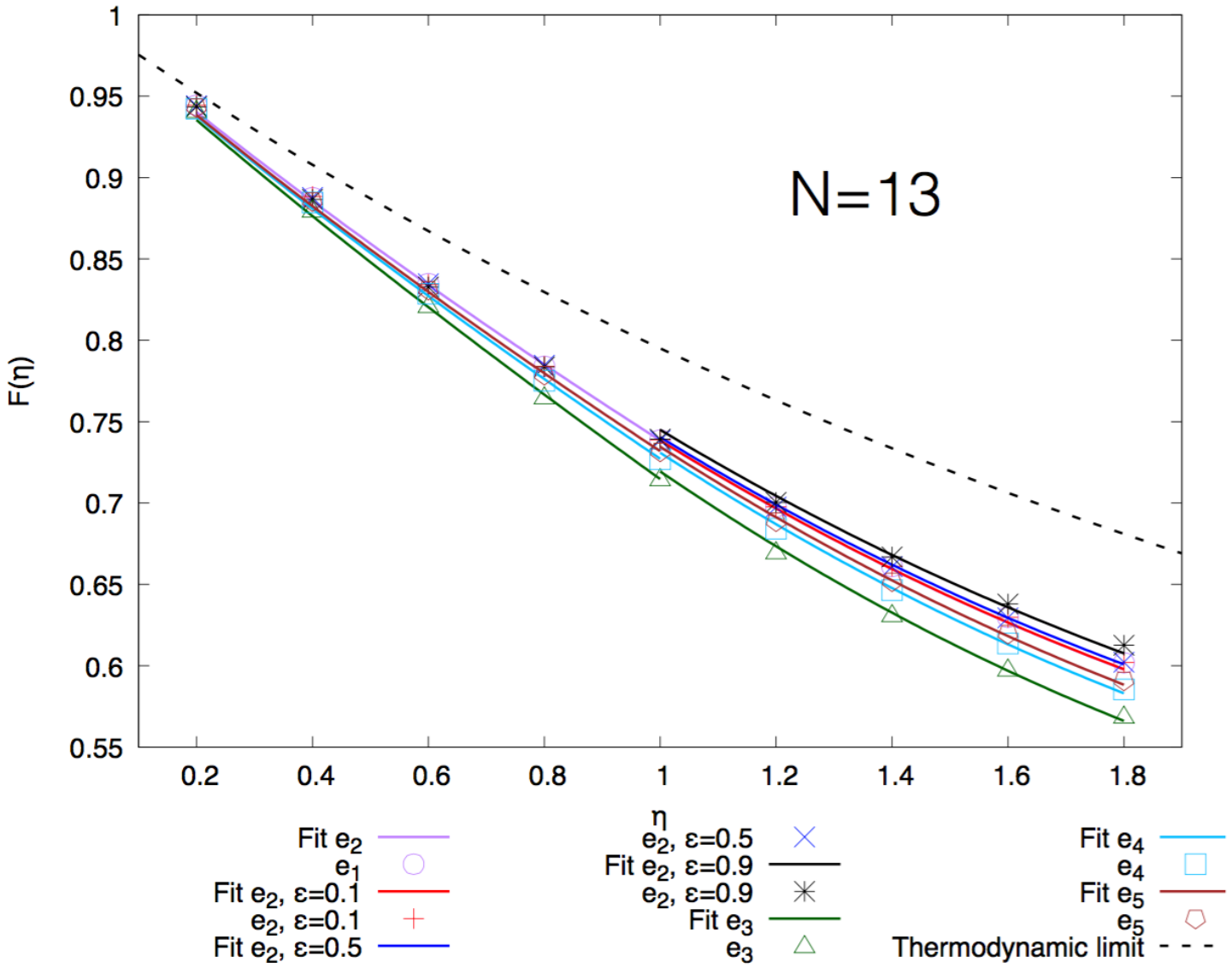
N=13
F(η)
η
1
0.95
0.9
0.85
0.8
0.75
0.7
0.65
0.6
0.55
0.2
0.4
0.6
0.8
1
1.2
1.4
1.6
1.8
Fit e2
e1
Fit e2, ε=0.1
e2, ε=0.1
Fit e2, ε=0.5
e2, ε=0.5
Fit e2, ε=0.9
e2, ε=0.9
Fit e3
e3
Fit e4
e4
Fit e5
e5
Thermodynamic limit

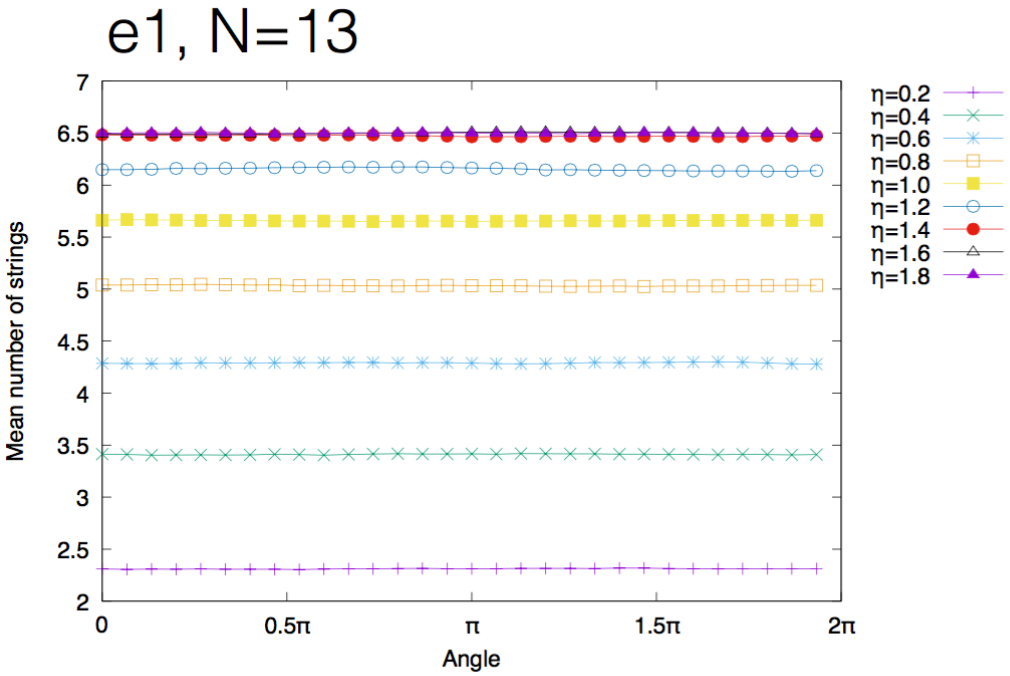
e1, N=13
Mean number of strings
Angle
7
6.5
6
5.5
5
4.5
4
3.5
3
2.5
2
0
0.5π
π
1.5π
2π
η=0.2
η=0.4
η=0.6
η=0.8
η=1.0
η=1.2
η=1.4
η=1.6
η=1.8

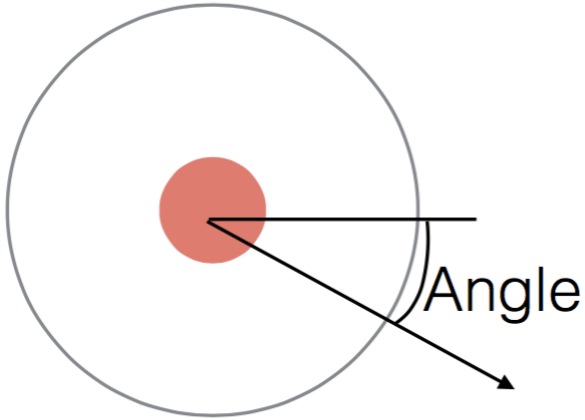
Angle

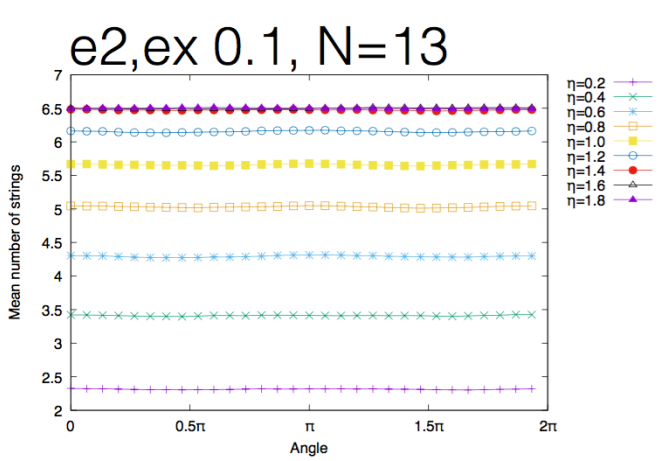
e2,ex 0.1, N=13
Mean number of strings
Angle
0
0.5π
π
1.5π
2π
η=0.2
η=0.4
η=0.6
η=0.8
η=1.0
η=1.2
η=1.4
η=1.6
η=1.8

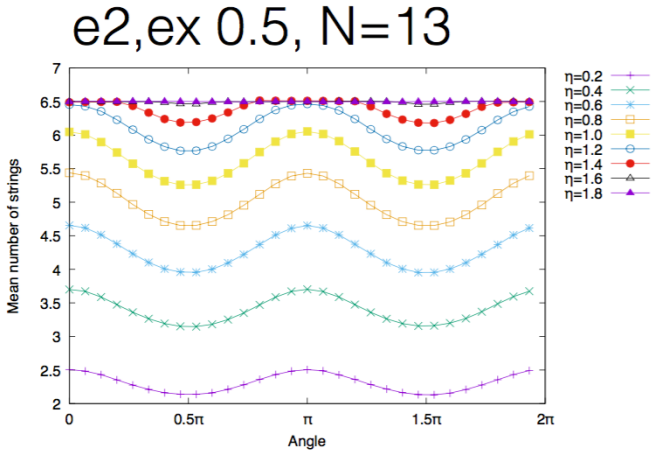
e2,ex 0.5, N=13
Mean number of strings
Angle
η=0.2
η=0.4
η=0.6
η=0.8
η=1.0
η=1.2
η=1.4
η=1.6
η=1.8

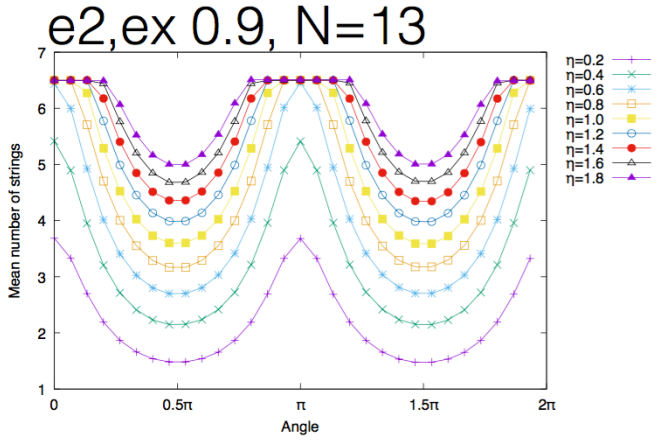
e2,ex 0.9, N=13
Mean number of strings
Angle
η=0.2
η=0.4
η=0.6
η=0.8
η=1.0
η=1.2
η=1.4
η=1.6
η=1.8

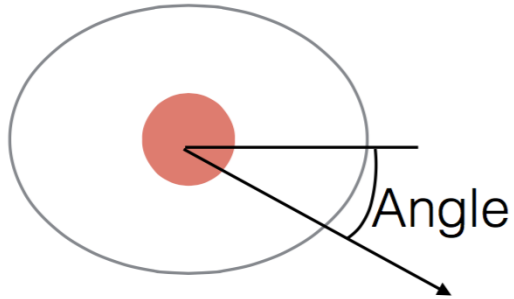
Angle

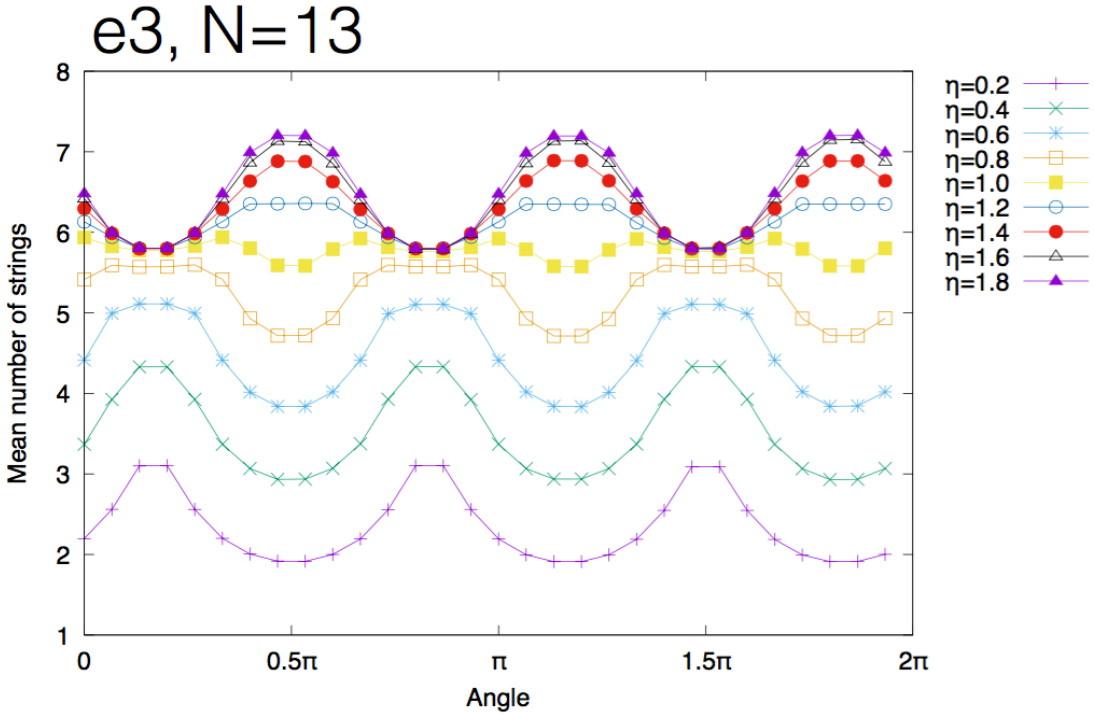
e3, N=13
Mean number of strings
Angle
0
0.5π
π
1.5π
2π
1
2
3
4
5
6
7
8
η=0.2
η=0.4
η=0.6
η=0.8
η=1.0
η=1.2
η=1.4
η=1.6
η=1.8

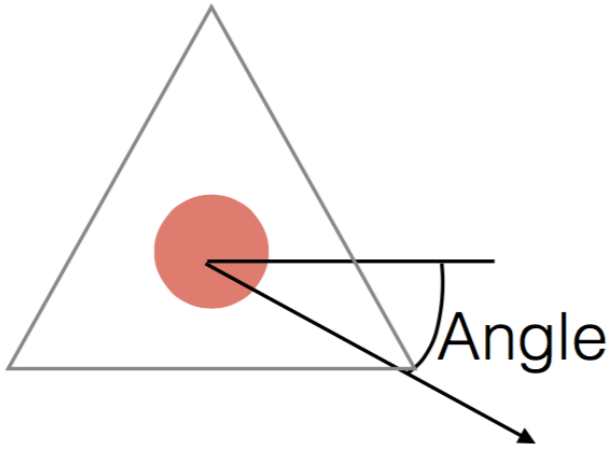
Angle

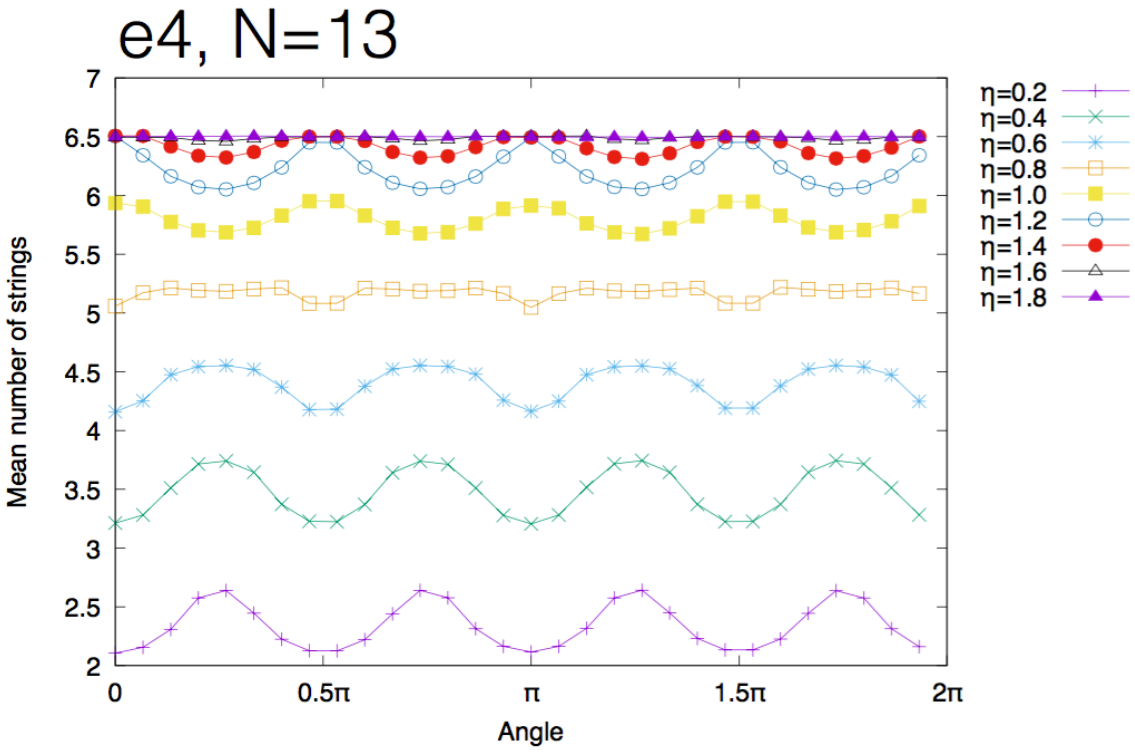
e4, N=13
Mean number of strings
Angle
0
0.5π
π
1.5π
2π
2
2.5
3
3.5
4
4.5
5
5.5
6
6.5
7
η=0.2
η=0.4
η=0.6
η=0.8
η=1.0
η=1.2
η=1.4
η=1.6
η=1.8

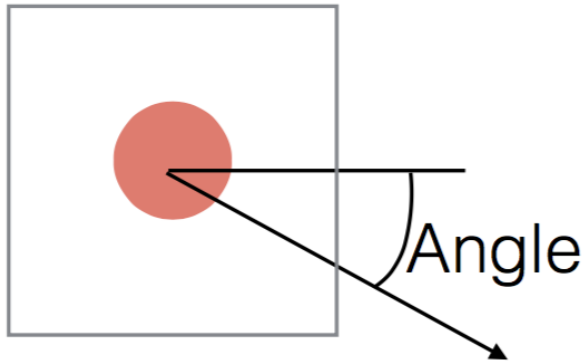
Angle

e5, N=13

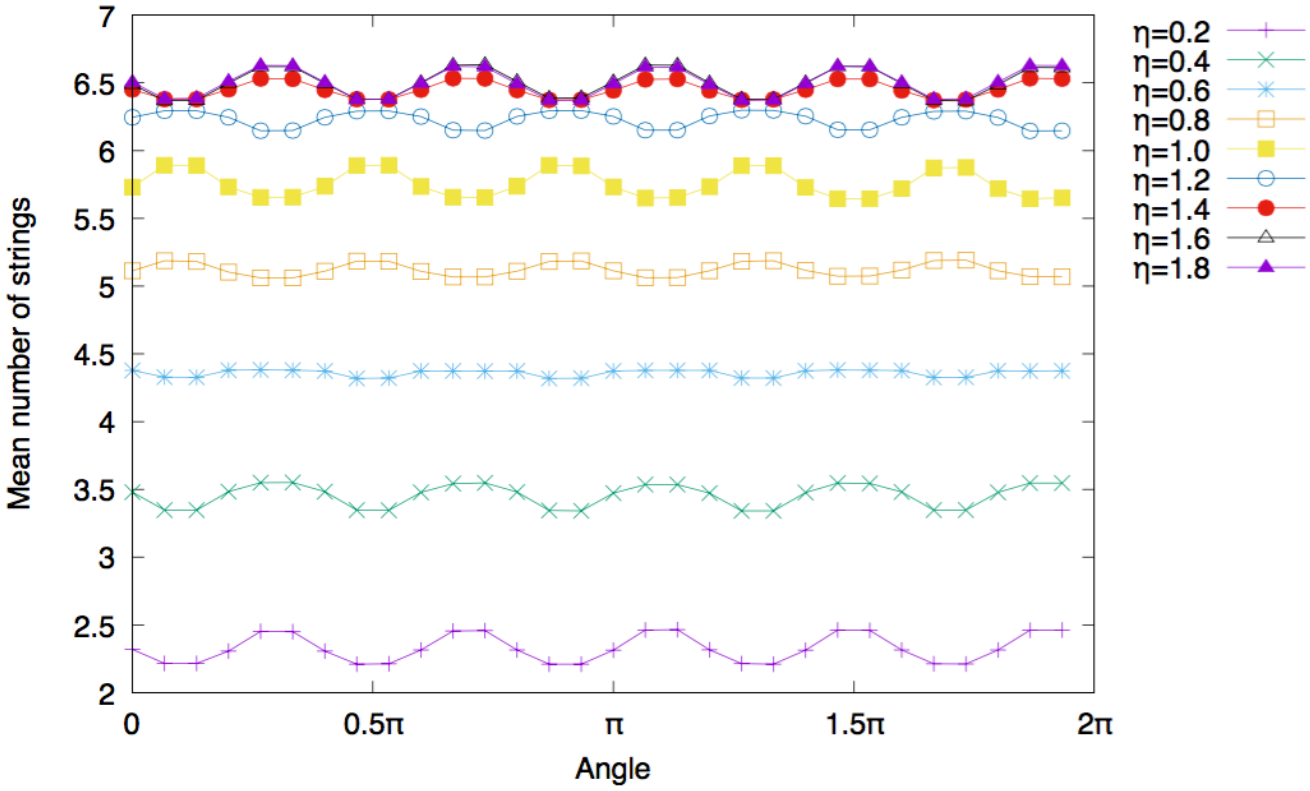
Mean number of strings
7
6.5
6
5.5
5
4.5
4
3.5
3
2.5
2
0
0.5π
π
1.5π
2π
Angle
η=0.2
η=0.4
η=0.6
η=0.8
η=1.0
η=1.2
η=1.4
η=1.6
η=1.8

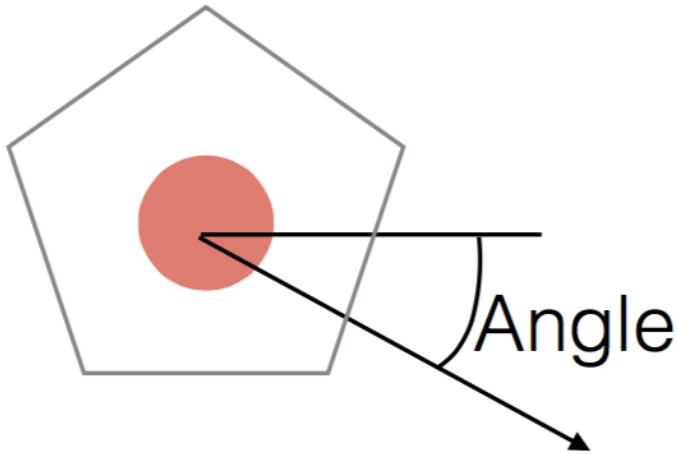
Angle

Onset near side ridge structure

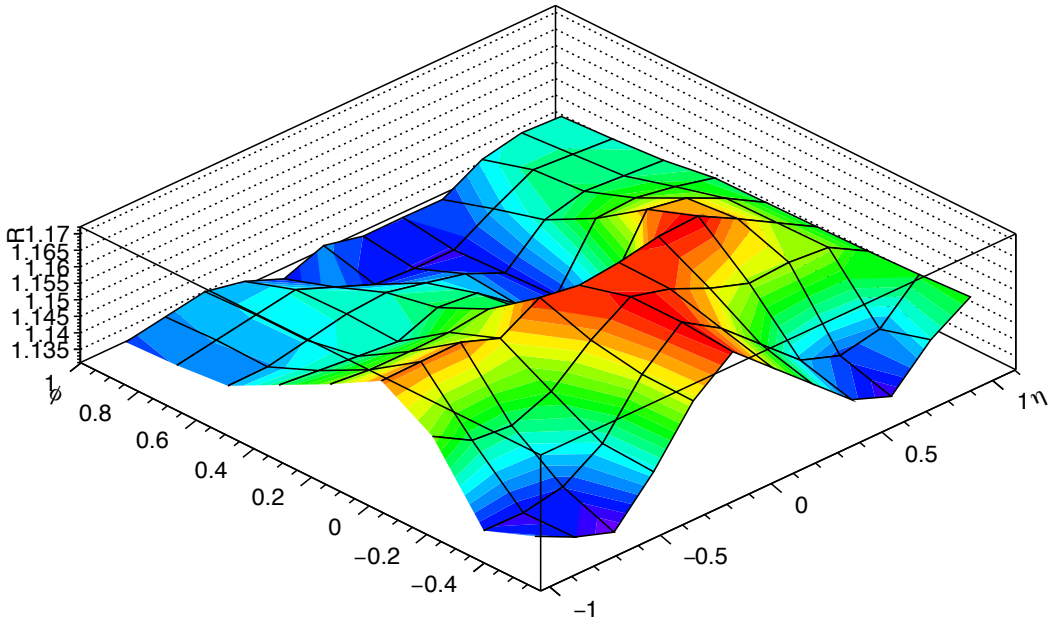

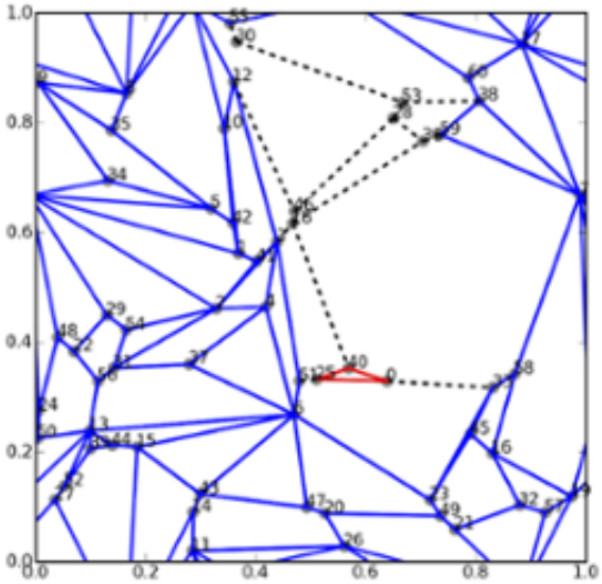

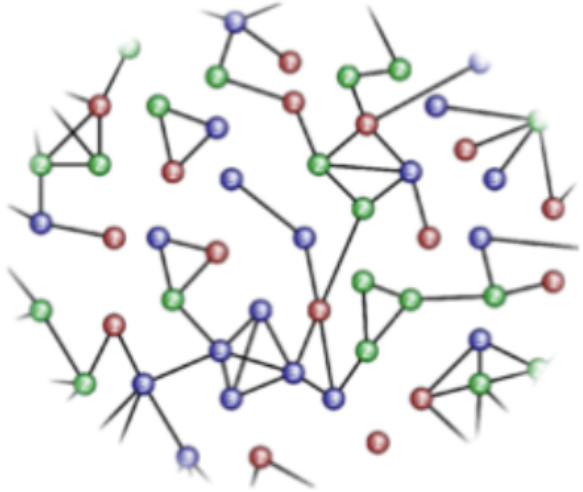

disordered systems -> often have fractal structure

lead to anomalous diffusive transport

dynamics of fluids in disordered media

In the framework of lattice models with randomly positioned defects

inhomogeneities are frequently not distributed totally at random but tend to be correlated over large distances. To understand the impact of this, it is useful to consider the limiting case where correlations decay asymptotically as a power law with distance
r : C(r)~r^a

If the correlation exponent a is smaller than the spatial dimension d,
the correlations are considered as long-range or “infinite”

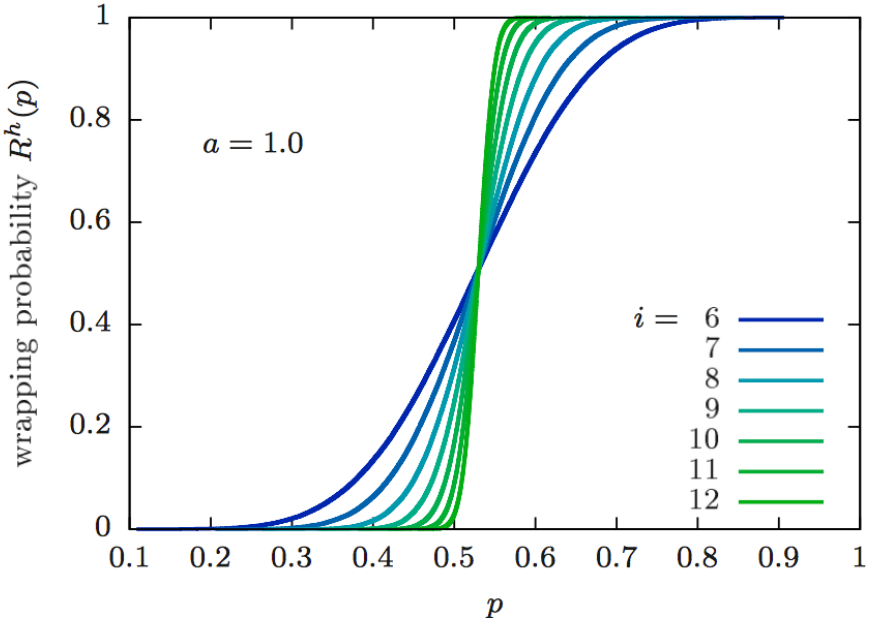

Example for finite-size scaling of the percolation threshold for a = 1 and lattice sizes L = 2i , i = 6, . . . , 12. Horizontal wrapping probabilities (left-hand) and critical concentrations (right- hand) obtained from the quenched disorder average of the occupation numbers

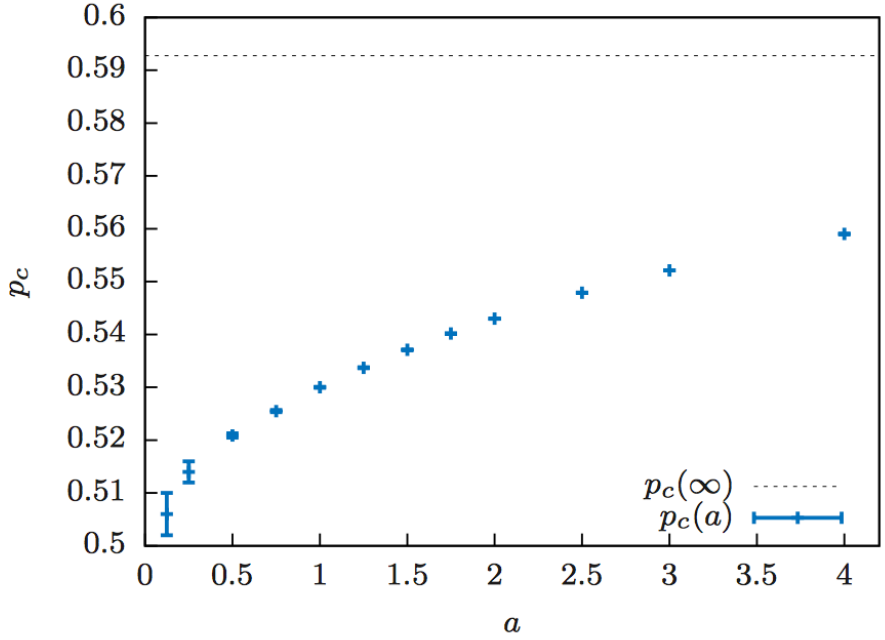

Blue line results of the percolation threshold pc from the finite-size scaling extrapolation as a function of the correlation strength for the square lattice. The dashed line indicates the value for the uncorrelated case which is recovered for a → ∞.

Phys. Rev. E 88, 052102 (2013)

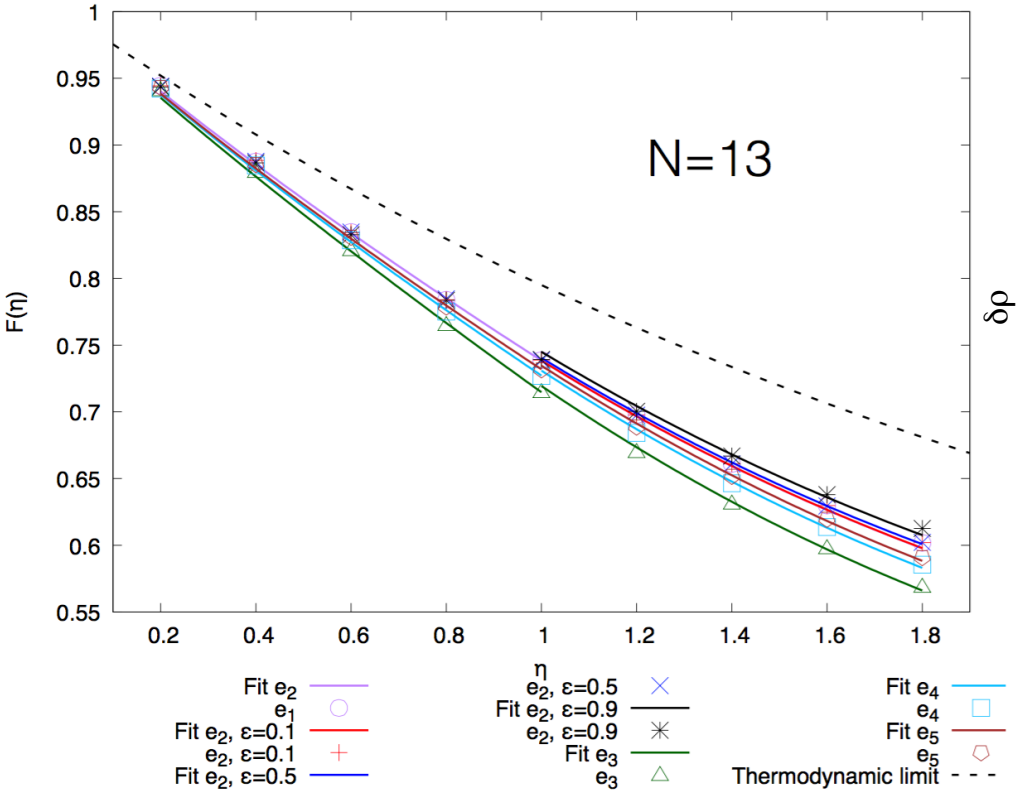

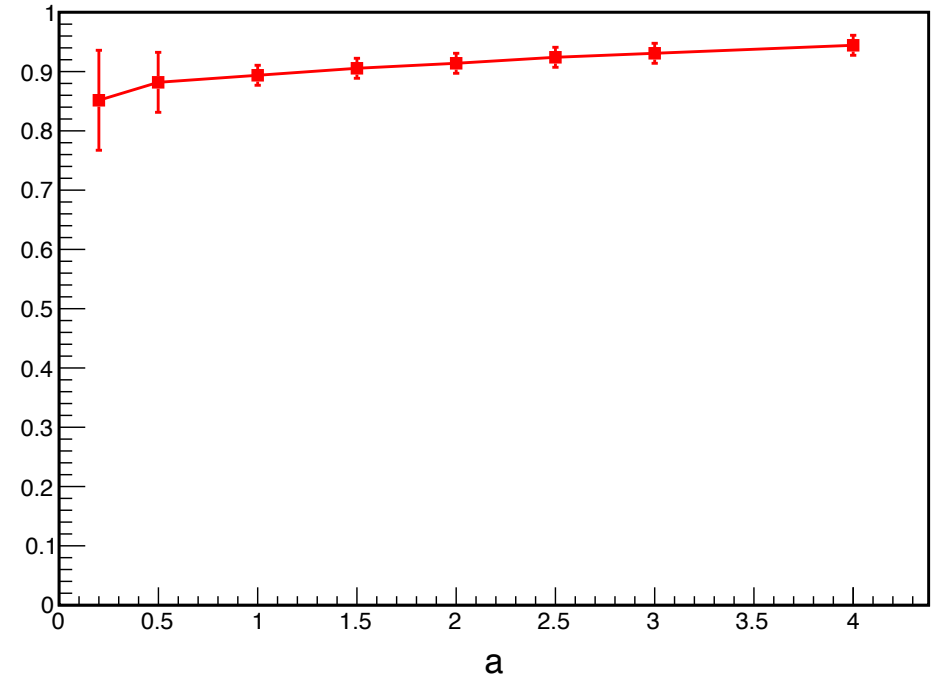

Results of the effects on the scaling function as a function of the correlation strength.

Onset near side ridge structure

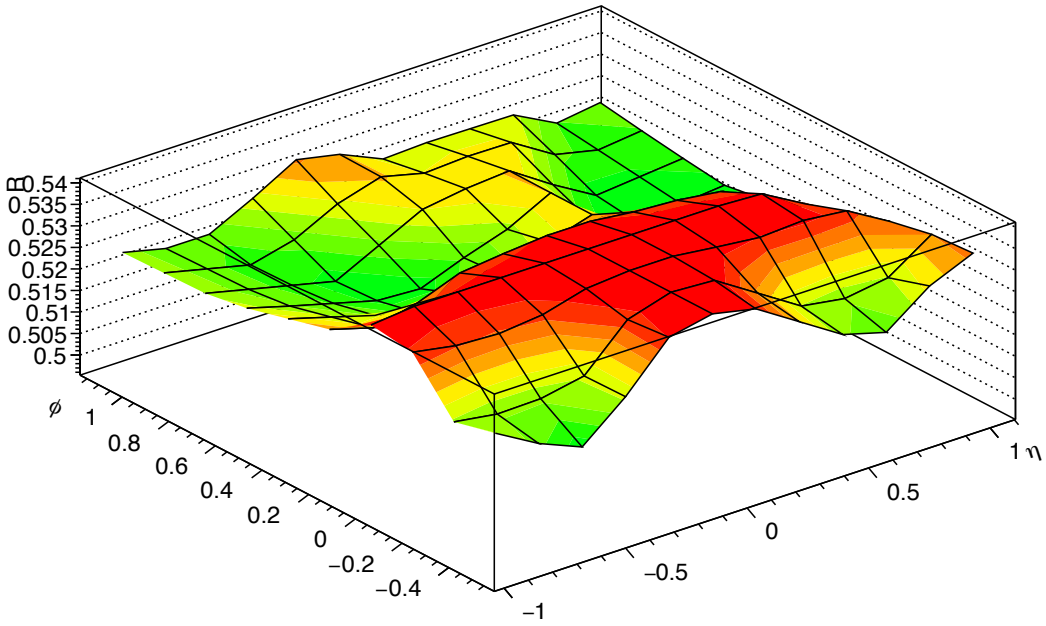

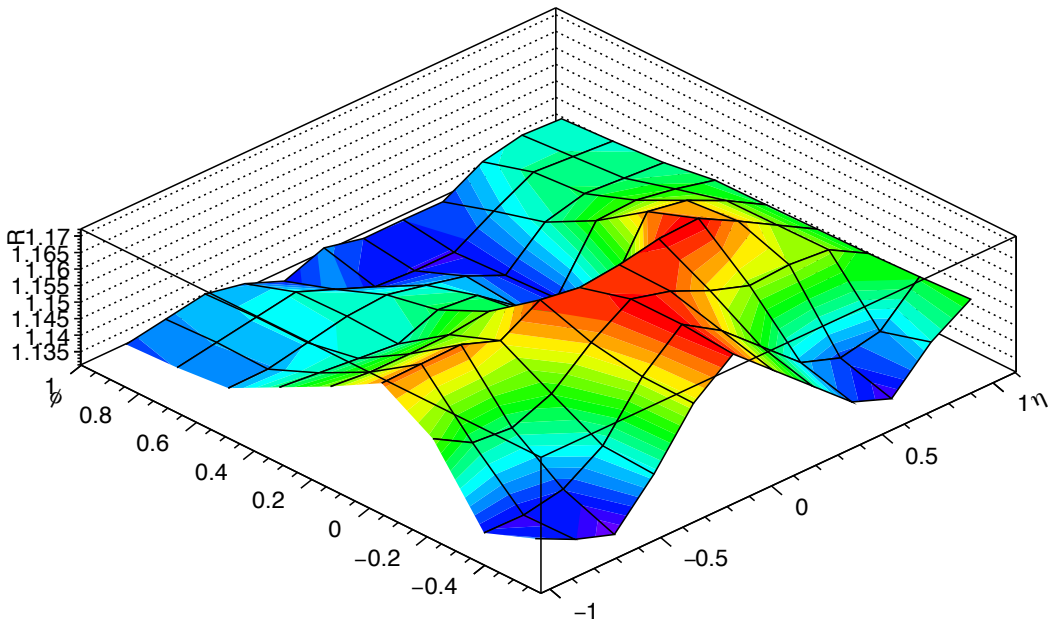

W/o correlation

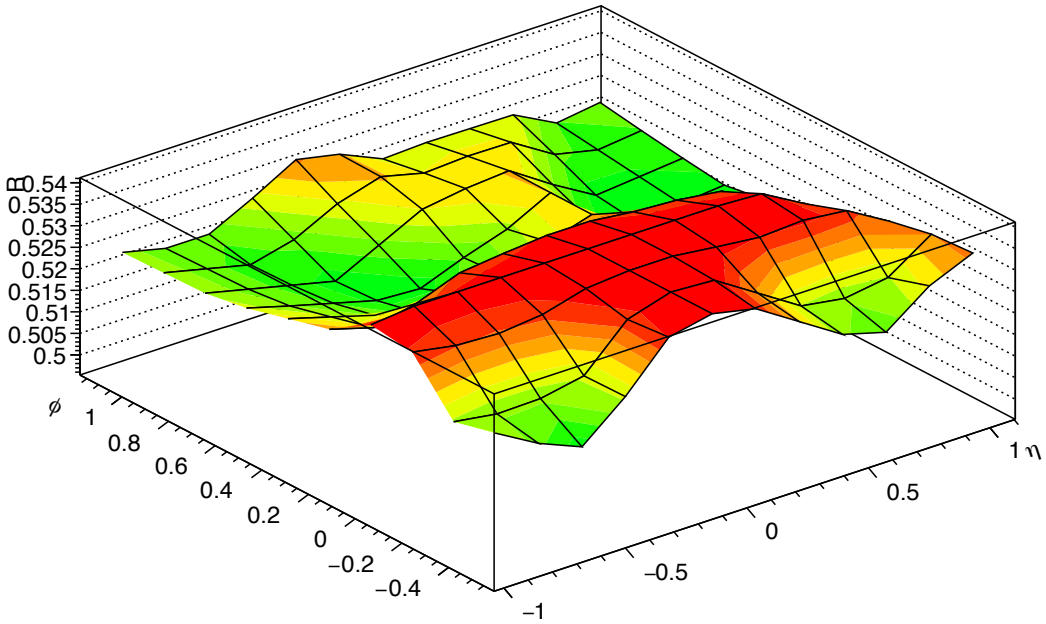

With correlation

Summary

- The onset near side ridge structure may be related to initial geometry fluctuations
- In our MC toy Model initial correlation contributes to the onset near side ridge structure.

Thank you!!

The 7th Conference on Large Hadron Collider Physics

May 20 - 25th, 2019

MEXICO, PUEBLA - BUAP

Website: lhcp2019.buap.mx

SPONSORED BY

INTERNATIONAL ADVISORY COMMITTEE

Torsten Åkesson (Lund University)
Charalampos Anastasiou (ETH Zurich)
Federico Antinori (INFN, Padua)
Pietro Antonioli (INFN, Bologna)
Gregorio Bernardi (LPNHE, Paris)
Florencia Canelli (Zurich University)
Roberto Carlin (University of Padova)
Heriberto Castilla Valdéz (CINVESTAV, Mexico)
Zaida Conesa del Valle (IPN, Orsay)
Ignacio Bediaga (CBPF, Rio de Janeiro)
Eckhard Elsen (CERN)
Paolo Giacomelli (INFN, Bologna)
Beate Heinemann (DESY, University of Freiburg)
Karl Jakobs (University of Freiburg)
Shan Jin (Nanjing University, Jiangsu)
Victor Kim (NRC KI - PNPI, Gatchina & SPbPU, St. Petersburg)
Leif Lönnblad (Lund University)
Marta Losada (Universidad Antonio Nariño)
Rohini Madhusudan Godbole (Indian Institute of Science, Bangalore)
Arturo Menchaca Rocha (UNAM, Mexico)
Guenakh Mitselmakher (University of Florida) Deputy Chair
Aleandro Nisati (INFN, Roma-I) Chair
Giovanni Passaleva (INFN, Firenze)
Monica Pepe-Altarelli (CERN)
Laura Reina (Florida State University)
Paris Sphicas (CERN & University of Athens)
Katsuo Tokushuku (KEK, Tsukuba)
Isabelle Wingerter-Seez (LAPP, Annecy)
Bolek Wyslouch (MIT, Cambridge)
Haijun Yang (SJTU, Shanghai)
Arnulfo Zepeda (CINVESTAV, Mexico)

SCIENTIFIC SECRETARIAT

Mario Iván Martínez Hernández (BUAP)
Pablo Roig Garcés (CINVESTAV, Mexico)

CONFERENCE CHAIRS

Irais Bautista (BUAP)
Arturo Fernández Téllez (BUAP)
Bruno Mansoulié (IRFU-CEA, Paris)
Jim Olsen (Princeton University)

TECHNICAL SECRETARIAT

Dawn Hudson (CERN)
Connie Potter (CERN)
Liliana Cortes (BUAP)
Maru Ordoñez (BUAP)
Misha Bautista (BUAP)

Contact: lhcp.2019@cern.ch

LHCP CONFERENCE 2019

PROGRAMME COMMITTEE

Simone Alioli (INFN, Milan Bicocca)
Ralf Averbeck (GSI, Darmstadt)
Tulika Bose (University of Wisconsin)
Tancredi Carli (CERN) co-Chair
Eduard de la Cruz Burelo (CINVESTAV, Mexico)
Dmitri Denisov (FNAL)
Luis R. Flores Castillo (Chinese University of Hong Kong)
Vladimir V. Gligorov (LPNHE, Paris)
Patrick Koppenburg (Nikhef)
Gabriel López Castro (CINVESTAV, Mexico)
Myriam Mondragón (UNAM, Mexico)
Antonio Ortiz Velásquez (UNAM, Mexico)
Shahram Rahatlou (Sapienza University & INFN, Roma) co-Chair
Veronica Sanz (University of Sussex)
Luca Silvestrini (CERN & INFN, Rome)
Marco van Leeuwen (Nikhef & CERN)
Urs Wiedemann (CERN)
Stephane Willocq (University of Massachusetts)

LOCAL ORGANIZING COMMITTEE

Alfredo Aranda Fernández (UCOL)
Irais Bautista (BUAP) co-Chair
Salvador Carrillo Moreno (IBERO)
Lorenzo Díaz Cruz (BUAP)
Jurgen Engelfried (UASLP)
José Feliciano Benitez (UNISON)
Olga G. Félix Beltrán (BUAP)
Arturo Fernández Téllez (BUAP) co-Chair
Iván Heredia de la Cruz (CINVESTAV, Mexico)
Martin Hentschinski (UDLAP)
Ildefonso León Monzón (UAS)
Mario Iván Martínez Hernández (BUAP)
Mauro Napsuciale Mendivil (U. Guanajuato)
Guy Paic (UNAM, Mexico)
Maria Isabel Pedraza Morales (BUAP)
Saúl Ramos Sánchez (UNAM, Mexico)
Mario Rodríguez Cahuantzi (BUAP)
Pablo Roig Garcés (CINVESTAV, Mexico)
Daniel Tapia Takaki (Kansas University & UNISON)
Guillermo Tejeda Muñoz (BUAP)